Leukocytic acetylcholine in chronic rejection of renal allografts

Joanna Wilczynska

INAUGURAL-DISSERTATION
submitted to the Faculty of Medicine
in partial fulfilment of the requirements
for the PhD-Degree
of the Faculties of Veterinary Medicine and Medicine
of the Justus Liebig University Giessen

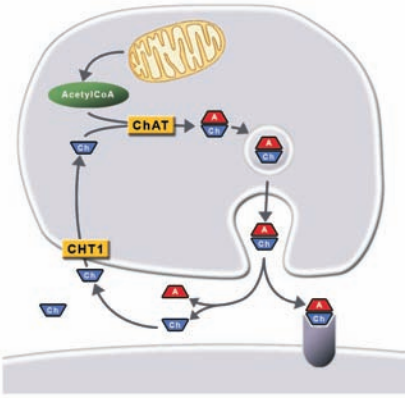

édition scientifique
VVB LAUFERSWEILER VERLAG

1. Auflage 2011

1st Edition 2011

Printed in Germany

édition scientifique
VVB LAUFERSWEILER VERLAG

STAUFENBERGRING 15, D-35396 GIESSEN
Tel: 0641-5599888 Fax: 0641-5599890
email: redaktion@doktorverlag.de

www.doktorverlag.de

Leukocytic acetylcholine in chronic rejection of renal allografts

Inaugural Dissertation

submitted to the

Faculty of Medicine

in partial fulfilment of the requirements

for the PhD-Degree

of the Faculties of Veterinary Medicine and Medicine

of the Justus Liebig University Giessen

by

Joanna Wilczynska

of

Sierpc, Poland

Giessen 2011

From the Laboratory of Experimental Surgery
Head: Prof. Dr. rer. nat. Veronika Grau
Department of General and Thoracic Surgery
Director/Chairman: Prof. Dr. med. Winfried Padberg

First Supervisor and Committee Member: Prof. Dr. Veronika Grau
Second Supervisor and Committee Member: Prof. Dr. Birgit Sawitzki
Committee Members: Prof. Dr. Norbert Weißmann
Prof. Dr. Heinz-Jürgen Thiel

Date of Doctoral Defence: 18th of August 2011

I TABLES OF CONTENT

II. LIST OF FIGURES

III. LIST OF TABLES

IV. LIST OF ABBREVIATIONS

ACh	acetylcholine
AChE	acetylcholinesterase
al.	alii
AP	alkaline phosphatase
APS	ammonium persulfate
Aqua ad inj.	aqua ad injectabilia
BChE	butyrylcholinesterase
bFGF	basic fibroblast growth factor
bp	base pairs
BSA	bovine serum albumin
CAI	chronic allograft injury
CAN	chronic allograft nephropathy
CarAT	carnitine acetyltransferase
CAV	chronic allograft vasculopathy
cDNA	complementary deoxyribonucleic acid
ChAT	choline acetyltransferase
ChE	cholinesterase
CHT1	high affinity choline transporter
DA	Dark Agouti
DAB	3,3'-diaminobenzidine
dH2O	distilled water
DI-water	deionised water
dNTP	deoxynucleotide triphosphate
EC	endothelial cells
ECM	extracellular matrix
EDTA	ethylenediaminetetraacetic acid
F433	Fischer 344
fwd	forward
GAPDH	glyceraldehyde 3-phosphate dehydrogenase
GBM	glomerular basement membrane
h	hour
HRP	horseradish peroxidase
IF	interstitial fibrosis

Ig	immunoglobulin
IL	interleukin
kDa	kilodalton
LEW	Lewis
mA	milliamper
mAb	monoclonal antibody
mAChR	muscarinic acetylcholine receptor
mRNA	messenger RNA
nAChR	nicotinic acetylcholine receptor
min	minute
MP	milk powder
NNK	nicotine-derived nitrosamine ketone; 4-(methylnitrosamino)-1-(3-pyridyl)-1-butanone
NO	nitric oxide
NOS	nitric oxide synthase
OCT	organic cation transporter
p. a.	pro analysi
PA	paraformaldehyde
PBGD	porphobilinogen deaminase
PBS	phosphate-buffered saline
PCA	peptide competition assay
PCR	polymerase chain reaction
PDGF	platelet derived growth factor
PVDF	polyvinylidene difluoride
qPCR	quantitative real-time polymerase chain reaction
rev	reverse
RNA	ribonucleic acid
RT	room temperature
RT-PCR	reverse transcription followed by PCR
s	second
SB	sample buffer
SDS	sodium dodecyl sulfate
SDS-PAGE	SDS-polyacrylamide gel electrophoresis
TA	tubular atrophy
TAE	tris-acetate-EDTA

TBS	tris-buffered saline
TG	transplant glomerulopathy
TGF	transforming growth factor
TPBS	PBS plus Tween® 20
V	volt
VAChT	vesicular acetylcholine transporter
VEGF	vascular endothelial growth factor
VSMC	vascular smooth muscle cells

1. Introduction

1.1 Kidney transplantation – graft loss and patient survival

Kidney transplantation is the current treatment of choice for patients with end-stage renal disease. Over the last 10 years, the number of kidney transplantations in the US has increased by 27% from 12 633 transplants in 1999 to 16 067 transplants in 2008 [1-2]. Although the number of transplantations per year may seem impressive, there is still a big difference between the number of donors and the number of patients on the waiting list (Figure 1.1) [2].

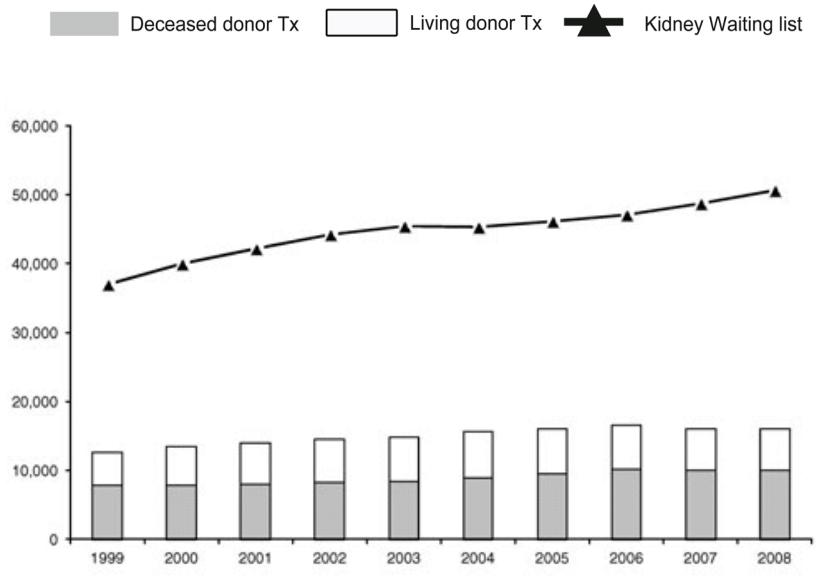

Figure 1.1 Number of kidney transplants between 1999 and 2008, and the number of patients on the waiting list. Tx, transplantation; [Source:[2]; with permission]

Improvement of the immunosuppressive therapy has resulted in a significant decrease in the incidence of acute rejection episodes after kidney transplantation and thus, in improving of the short term graft survival [3]. Basing on the US kidney transplantation report from the period between 1998 and 2007, we can observe that the one year graft survival increased from 89% in 1998 to 91% in 2007 for deceased donors and from 95% in 1998 to 97% in 2007 for living donors [2]. Although the long-term allograft survival has also improved, the annual rate of graft loss remains relatively high. For kidney transplants performed before 2007, graft survival was best for recipients of living donor kidneys, intermediate for non-expanded criteria donor and lowest for expanded criteria donor transplants. Patient survival followed the same pattern (Figure 1.2) [1-2, 4-5].

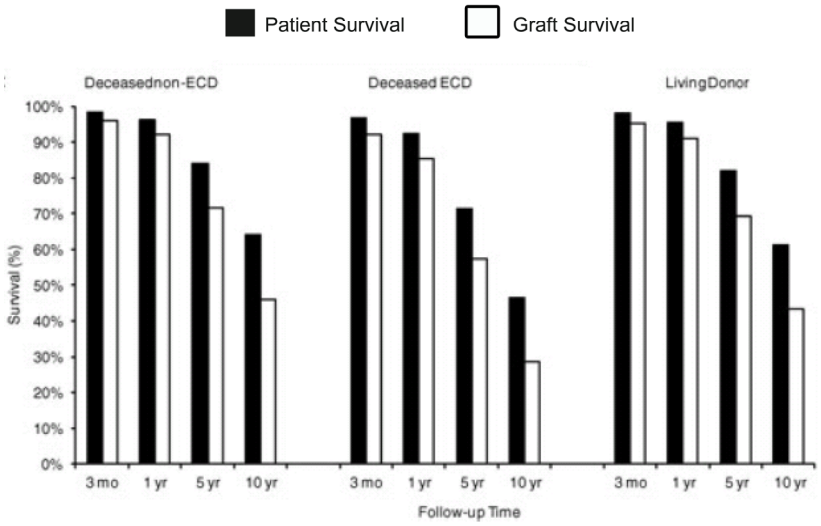

Figure 1.2 Patient and renal graft survival by donor type. Three months, one year (for transplantations during 2006-2007), 5-year (for transplantations during 2002-2007) and 10-year (for transplantations during 1997-2007) follow-up time. ECD - expanded criteria donor. [Source:[2]; with permission]

It is of importance to identify the risk factors, which influence the long-term graft survival, to improve immunosuppressive therapy and post transplant care.

1.2 Allograft rejection

Organs undergoing acute rejection are infiltrated by host leukocytes, which cause graft cell necrosis and vessel thrombosis. Clinically, the commonly used immunosuppressive agents prevent or reverse most acute rejection episodes [6]. However, acute rejection episodes, even when completely reversed, are important risk factors for the development of chronic allograft rejection [7-9]. The estimated half-life of the transplanted organ is much lower in patients who underwent acute rejection episodes (6.6 years) than those who did not (12.5 years) [10]. It has been shown that the type of acute rejection, its timing and the number of acute rejection episodes play an important role in future development of chronic rejection [10], however, the contribution of the severity of acute rejection episodes to chronic rejection remains unclear [11]. The occurrence of an acute rejection episode within the first three months after transplantation is very common. It can be diagnosed in over 83% of renal grafts and does not necessarily influence the long-term graft outcome [12]. Acute rejection episodes between the 2nd and the 6th months after transplantation however, can be a risk factor for the development of histopathological lesions in the grafts [13]. Despite the use of immunosuppression and

correct transplant aftercare, more than 21% of patients experience more than one acute rejection episode during the first posttransplant year [12].

Chronic renal rejection is the principal cause of long-term graft failure, and occurs in 50% to 80% of the patients who return to dialysis after transplantations [14]. It develops over months and leads to graft loss in a period of years. It is defined by chronic allograft vasculopathy (CAV), transplant glomerulopathy (TG), tubular atrophy (TA), and/or interstitial fibrosis (IF) [9, 15-21].

1.2.1 Chronic allograft vasculopathy (CAV)

CAV is one of the causes of long-term dysfunction of the allograft. The process of development is well described and similar for the heart (the abbreviation CAV is also used for cardiac allograft vasculopathy or coronary allograft vasculopathy) and for the kidney [22-25]. CAV is characterised by progressive fibrointimal thickening of arteries, arterioles and glomerular tufts [20, 25-26] and can be observed in the allograft as early as one month after transplantation [27-28]. Thickening of the arterial wall is caused by infiltrating inflammatory cells (macrophages, lymphocytes), proliferating vascular smooth muscle cells (VSMC) [22] and myofibroblast, which accumulate in the intima, as well as by duplication or breaking of the internal elastic membrane [25], and finally, endothelial cell (EC) proliferation [29]. It reduces the blood flow in the organ and contributes to TG and tubulointerstitial lesions, which result in late allograft damage and failure [30]. In the pathophysiology of CAV, both immunologic factors (acute rejection episodes, chronic inflammation, hypertension, etc.) and non-immunologic factors (age, sex of the donor, smoking, ischemia-reperfusion injury, etc.) play a role [23-24]. It has been proposed that damage and apoptosis of EC may initiate the fibrointimal changes characteristic for CAV [31]. During chronic renal rejection, T-cell and antibody dependent pathways play a role in destruction of the allograft cells [25]. The vascular EC layer is the first component challenged by the immune system of the recipient [25] (Figure 1.3).

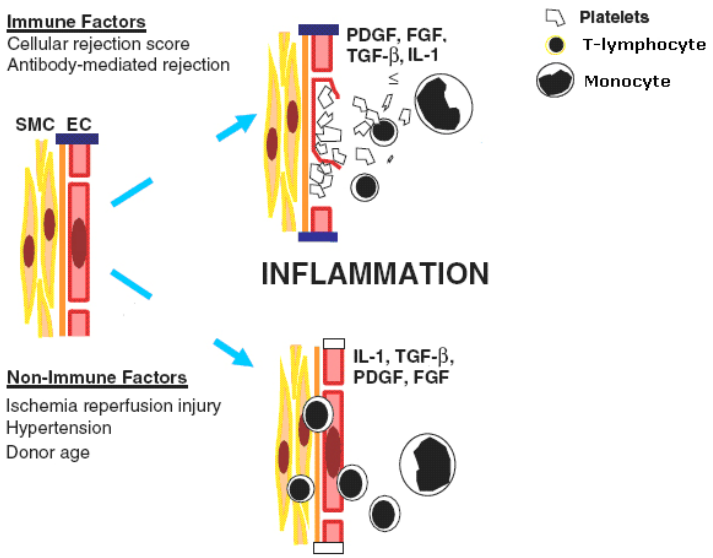

Figure 1.3: **Mechanisms triggering allograft vasculopathy.** Allograft vasculopathy can be caused by both immunological and non-immunological factors. EC, endothelial cells; FGF, fibroblast growth factor; IL, interleukin; PDGF, platelet-derived growth factor; SMC, smooth muscle cell; TGF-β, transforming growth factor-β; [Source: [24]; with permission].

Disruption of the EC monolayer results in attachment and adherence of platelets circulating in the blood stream. They release platelet-derived growth factor (PDGF), which causes VSMC migration and proliferation at the place of injury [32]. Next, leukocytes (mainly monocytes) are attracted. They secrete numerous cytokines and growth factors like vascular endothelial growth factor (VEGF), PDGF, basic fibroblast growth factor (bFGF), transforming growth factor-α and -β (TGF-α, TGF-β) or interleukin-1 (IL-1), which also promote VSMC proliferation and migration to the intima [29]. In normal arteries, the extracellular matrix (ECM) prevents VSMC from migration, however, after injury, the ECM undergoes changes to allow cell movement. Finally, proliferation of EC allows rebuilding the endothelial layer, which was damaged upon injury.

It has been shown that the thickness of the arterial intima increases four months after transplantation, but no further changes were observed on follow-up biopsies one year after transplantation [33]. CAV significantly decreases the long term graft survival (41% vs. 82% in patients with chronic allograft nephropathy (CAN) but without vessel narrowing) [34].

1.2.2 Transplant glomerulopathy (TG)

TG is another pathological condition of renal allografts associated with very poor allograft survival [15]. TG is rarely diagnosed during first 6 months after transplantation but the probability is increasing to 4% during the first year, and to over 20% after 5 years [19]. It is commonly observed in patients with ongoing acute rejection or with a history of acute

rejection episodes (54% of TG positive biopsies were obtained from patients with a history of acute rejection). TG can be easily observed by light and electron microscopy [15-16, 19, 26]. The most characteristic lesion for TG is thickening or doubling of the glomerular basement membrane (GBM). It can be seen after Periodic acid-Schiff and/or silver staining of kidney sections [15]. Less specific changes (which can occur not only in TG) include partial or global sclerosis or enlargement of glomeruli, which is an effect of increased size of endothelial and mesanglial cells, infiltration of the glomeruli with mononuclear cells and loss of continuity in GBM [9, 26]. Early TG does not necessary affect all glomeruli in the kidney [15]. Clinically, TG is characterised by proteinuria, progressive reduction of graft function and hypertension [35]. A reduced glomerular filtration rate between 6 and 12 months is associated with the development of chronic rejection after 12 months [36].

1.2.3 Tubular atrophy (TA) and interstitial fibrosis (IF)

IF and TA are common signs of progressive loss of graft function, especially when observed together with CAV and TG. Tubular epithelial cells and tubulointerstitial fibroblasts may be damaged during organ inflammation or injury [17, 37]. Together with patchy fibrosis of the interstitium and atrophy of the tubules, there is infiltration by lymphocytes and macrophages [18]. The basement membrane of the tubules is thickened and/or duplicated, and peritubular capillaries disappear. In atrophic tubules, intratubular mononuclear cells can be seen. Numerous risk factors have been correlated with the development of IF/TA during the first year after transplantation. They are similar to the risk factors connected with TG or CAV and include ischemia-reperfusion injury, donor age and previous episodes of acute rejection [18]. In kidney biopsies, tubulointerstitial changes were diagnosed already 6 weeks after transplantation in 5% of grafts, at three months in 11% [38], at 4 to 6 months between 37 and 40% [38-39], and at one year in approximately 50% of the grafts [40]. Clinically, IF/TA scoring is more commonly used than TG or CAV scoring. In small biopsy cores, there is frequently more tubulointerstitial space than glomeruli or arteries, which can be investigated [18]. It is also possible to quantify precisely the area of IF by histomorphometry [41].

1.3 Experimental models for chronic renal allograft rejection

The most commonly used model to study chronic renal allograft rejection is transplantation in the Fischer 344 (F344) to Lewis (LEW) rat strain combination [42-43]. It was first described by White *et al.* in 1969 [44]. The F344 ($RT1^{lvr}$) rat has a variant *l* haplotype that differs from LEW ($RT1^{l}$) in the major histocompatibility complex class I E/C region but is

identical to LEW in the immunodominant RT1.A and RT1.B regions [45]. This model allows to analyse the progression of chronic rejection which is characterised by slow reduction of the functions of the organ [46]. The renal grafts survive over 60 weeks and develop typical histological changes comparable with CAN [44]. At 4 weeks after transplantation, mononuclear cell infiltration, thickening of the GBM and proliferation of the mesanglial cells are observed. At 12 weeks, the mononuclear infiltration of the vessel walls is increased along with progressive damage of the glomeruli (together with further thickening of the basement membrane). The tubular basement membrane is also thickened. At 28 weeks, there are clear sings of IF and CAV – with intimal hyperplasia and disruption of internal elastic lamina [44]. At present, this model is widely used. In most studies, the immunosuppressive drug – cyclosporine – is administered to the animals for 10 days after transplantation [44].

The F344 to LEW rat strain combination is also used in this study to investigate chronic rejection of renal allografts, however, no immunosuppression is given after transplantation. Renal allografts in LEW recipients develop all functional and histological symptoms of CAN, which are described for human renal grafts. It has already been shown that after transplantation in the F344 to LEW rat strain combination. Reversible acute rejection developes and mononuclear leukocytes accumulate in the blood vessels of renal allografts and the cell number peaks around day 9 post-transplantation [47].

1.4 From acetylcholine (ACh) to CAV

1.4.1 ACh in fatal acute rejection

Previous studies in our laboratory focused on fatal acute rejection. Allogeneic transplantations were performed in fully allogeneic Dark Agouti (DA) to LEW rat strain combination and isogeneic transplantation in LEW to LEW rat strain combination. Numerous leukocytes accumulate in the lumen of the blood vessels of the allografts before irreversible destruction of the organ (between days 4 and 5) [47-48]. 14% of these cells are T-cells and over 70% are activated monocytes, which have proinflammatory properties [49-50]. In renal isografts, the cell population consists of about 50% of mildly activated monocytes [49]. The presence of ACh and the enzymatic machinery for its synthesis (choline acetyltransferase (ChAT) and high affinity choline transporter (CHT1) has been shown before in blood lymphocytes of both rats and humans. They are considered as a major source of non-neuronal ACh in the blood [51-55]. Moreover, it has been shown that mononuclear monocytes, which accumulate in the graft vessels during fatal acute rejection are a source of

ACh [48]: ChAT and CHT1 mRNA and proteins are upregulated upon acute allograft rejection. Additionally, immunohistochemical analysis revealed that numerous intravascular monocytes are positive for ChAT and CHT1 proteins [48].

1.4.2 ACh in vascular remodelling

The importance of CAV in the progression of chronic allograft rejection is known and well described (1.2). Moreover, there are hints that interactions of accumulated blood leukocytes in the vessels of the allograft with vascular endothelial cells play an important pathogenic role for the development of CAV [25, 49-50, 56-59]. Interestingly, EC, SMC and immune cells are among several non-neuronal cell types, which produce ACh [60], a factor involved in cell proliferation, differentiation and intercellular communication [60].

1.4.3 ACh and nicotine – ligands for nicotinic ACh receptors

Both EC and VSMC express nicotinic (nAChR) and muscarinic (mAChR) cholinergic receptors. Several studies have indicated the role of nAChRs in cell proliferation and angiogenesis, which suggests their involvement in the process of vascular remodelling [61-63]. ACh is the physiological ligand for nAChRs, however, nicotine and NNK (nicotine-derived nitrosamine ketone, a tobacco smoke component) are also high affinity agonists of the nAChRs [61].

nAChRs are ligand-gated ion channels, built from five subunits. The variety of the subunits (9 α, 4 β, γ, δ and ε) allows formation of receptors with different functions and affinities to ligands [64]. The structure of all subunits is similar and includes an extracellular domain (N-terminal), four transmembrane domains, one intracellular domain, and a small extracellular domain (C-terminal). ACh and other agonists bind to the N-terminus [65]. It has been demonstrated that the proliferative and angiogenic effects of nicotinic agonists are mediated by α7-nAChRs [63].

It is known that tobacco smoking is associated with many pathologies of the blood vessels, like peripheral vascular diseases, which result in a reduction in vascular density and decreased vessels diameter [66-67]. Nicotine is the major addictive and best known tobacco component. Although nicotine has not been shown to be carcinogenic by itself, several studies show that nicotine or nicotine derivatives (e.g. NNK) enhance proliferation of endothelial cells via α7-nAChRs and induction of growth factors [66, 68-72]. If nicotinic stimulation of endothelial cells results in pro- or antiinflammatory effects is still disputed.

Antiinflammatory effects were reported for stimulation of endothelial α7-nAChR [73-74]. In contrast, long-term treatment with nicotine results in arterial inflammation and atherosclerotic lesions. This is at least in part due to a direct induction of prothrombotic tissue factor expression by endothelial cells [75] but also to indirect effects mediated by dendritic cells and macrophages [76-77].

Nicotine enhances the expression of many important growth factors and mediators of angiogenesis. VEGF expression is induced by nicotine in cancer [66, 78-80]. This effect is mediated by nAChRs. Treatment with mecamylamine, an inhibitor of nAChR, reduces plasma levels of VEGF in animals with tumor [81]. Nicotine has been shown to increase the VEGF receptor 2 expression in EC from angiogenic vessels [66, 78-79, 82]. This effect can be inhibited by the nAChR antagonist, hexamethonium [83]. bFGF, PDGF, TGF-β, factors which promote SMC proliferation, can also be up-regulated by nicotine [84-85]. Nicotine induces the secretion of prostacycline, which is connected with EC survival and migration. Prostacycline can also promote VEGF and FGF mediated angiogenesis [86-87]. Nicotine has been shown to increase the release of endothelin from EC [88]. Under certain conditions, endothelin can work as a proangiogenic factor [89-90]. Among other antagonists of nAChRs there are mecamylamine a non-selective antagonist, which has been shown to inhibit the endothelial network formation during *in vitro* studies on angiogenesis [84] and α-bungarotoxin, an antagonist of nAChRs, which has been shown to inhibit tube formation of endothelial cells *in vitro* [62].

1.4.4 ACh synthesis in non-neuronal cells

ACh is synthesised from acetyl-CoA and choline with the help of ChAT (Figure 1.5). While acetyl-CoA is produced in mitochondria, choline has to be transported from extracellular space. It is the rate-limiting step of the synthesis, which depends on CHT1. In the absence of ChAT, an alternative enzyme - carnitine acetyltransferase (CarAT) - can be used to synthesise ACh. Storage and release of ACh is mediated in neurons by the vesicular ACh transporter (VAChT), which is not an essential component of non-neuronal cholinergic cells. However, there is evidence of ACh release via polyspecific organic cation transporters (OCTs) 1, 2 and 3 [91-92]. After releasing, ACh is rapidly hydrolysed by acetylcholinesterase (AChE) or butyrylcholinesterase (BChE) into choline and acetate [93-94].

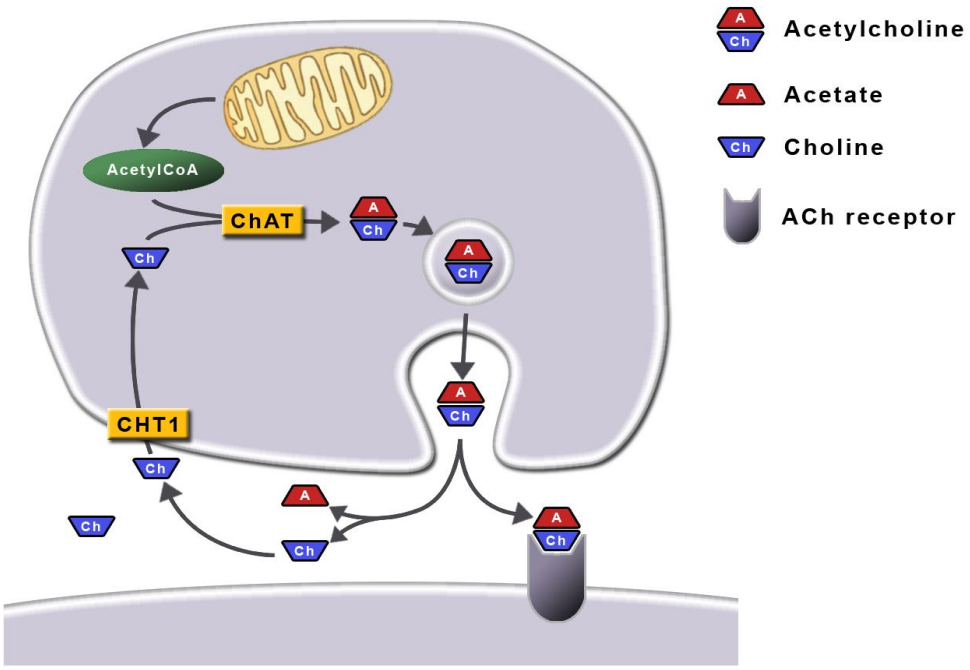

Figure 1.4: **ACh synthesis and recycling in non-neuronal cells.** CHT1, high affinity choline transporter; ChAT, choline acetyltransferase; Acetyl-CoA, acetyl coenzyme A; A, acetate; Ch, choline; ACh, acetylcholine.

1.4.4.1 Choline acetyltransferase (ChAT) gene and protein

ChAT is a globular protein with apparent molecular weight of 68 kDa (68 kDa in human and pig neuronal tissue, 67 kDa in rat neuronal tissue) [95]. However, isoforms of ChAT with a different molecular mass can be produced due to the alternative splicing (82 kDa variant of neuronal ChAT in humans; 67, 54 and 13 kDa in *Drosophila*; 41 and 54 kDa in human airway epithelial cells) [96-99]. In some species, the molecular weight of ChAT is lower than the predicted one (calculated from amino acid sequence form cloned cDNA). The difference could be due to post-translational modifications [95]. In all species investigated, ChAT is a product of a single gene (which also encodes VAChT within the first intron). Although there is high similarity in coding regions of ChAT nucleotide sequences of human, rat, mouse and pig, there are differences in non-coding regions [100]. A variety of mRNA species has been identified in mouse (R1-R4, N1-N2, M) rat (R1-R2, N1-N2, M) and human (R2, N1-N2, M) (Figure 1.6) [100-102].

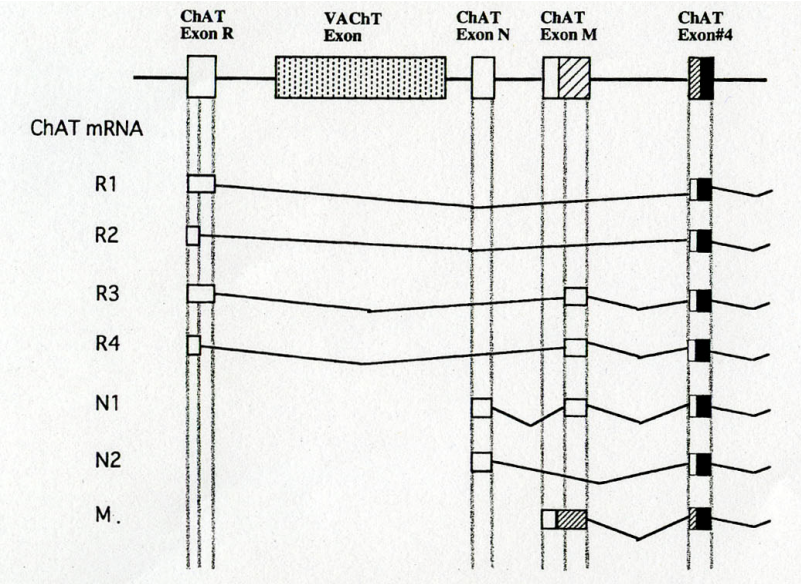

Figure 1.5: **Splicing patterns of different ChAT mRNA species** [Source: [95]; with permission]. ChAT, choline acetyltransferase; (■), common coding region of ChAT; (□), non-coding regions; (▨), possibly translated regions in human M-type only; R1-R4, N1-N2, M, non-coding exons.

ChAT in human nerve terminals exists in two forms – a soluble (80-90% of the enzyme activity) and a membrane-bound form (10-20%) [103-104]. Besides the central and the peripheral nervous system, ChAT expression has been found in numerous mammalian cells, like epithelial cells (airways, intestine, epidermis, stomach, kidney pelvis, urinary bladder), endothelial cells (veins, vessels) and in immune cells (lymphocytes, alveolar macrophages, granulocytes, monocytes), including 13 human leukemic cell lines [48, 53, 93, 105-107]. In B-cell lines, a weak activity of the enzyme was detected, but no ChAT mRNA was found [108].

ChAT has a high specificity for choline, but is less specific for acetyl-CoA and shows equal affinity for propionyl-CoA and butyryl-CoA. Besides ACh, ChAT can synthesise propionylcholine and butyrylcholine [109]. The ACh content in lymphocytes has been shown to correlate with ChAT activity and after lymphocyte stimulation, the ChAT activity is increased [110]. Casein kinase II as well as protein kinase C can increase ChAT activity [111]. Nerve growth factor has also been reported to increase ChAT activity, which increased ACh release [112].

1.4.4.2 Carnitine acetyltransferase (CarAT)

CarAT also belongs to the family of choline/carnitine acetyltransferases. It is a mitochondrial enzyme, which participates in ACh synthesis in the peripheral nervous system. Although CarAT has been reported to be expressed in lymphocytes, its expression did not correlate with ACh synthesis [110], which suggested a minor role in the process. In contrast, *Lips et al*. [113] has shown that in the absence of ChAT mRNA in human urothelium, CarAT is the main enzyme responsible for ACh synthesis. CarAT has also been detected in some human leukemic cell lines together with ChAT. The enzyme activity varies between cell lines, but without any correlation with ACh synthesis [107].

1.4.4.3 High affinity choline transporter (CHT1) and choline transport

Choline transport is one of the crucial processes for the function of all cells. Besides being a key element for ACh synthesis, it is needed for the synthesis of membrane phospholipids and signaling lipids [114-115]. There are two essential choline transport systems inhibited by hemicholinium-3 (HC-3): low-affinity (sodium independent), and high-affinity (sodium and chloride dependent) [116]. The high affinity choline transport was reported primarily in cholinergic neurons and proved essential for the ACh synthesis [117]. The inhibition of high affinity choline uptake with HC-3 reduced the cholinergic function [118]. The genes for non-neuronal CHT1 were cloned for the first time by Okuda *et al.* in 2000 [119] from *C. elegans* and rat and proved to have the same characteristics as CHT1 in cholinergic nerve endings. Human, mouse, *Limulus* and *Torpedo* CHT1 genes have been isolated thereafter [120-123]. Rat CHT1 gene has the highest homology to mouse CHT1 (98%) and human CHT1 (93%), and less to other investigated species (from 52-72%) [124]. The 580 amino acid protein is a member of sodium dependent glucose transporter family [120, 123-124]. Although its sequence has about 25% identity to other members of the transporter family, it shows no similarities to the known neurotransmitter transporters [121-122, 124]. Later on, CHT1 has been detected in several non-neuronal cells, where it has been localised in the membrane: epithelial cells of human and rat skin, rat trachea, brain, lung, arterial smooth muscle cells, fibroblasts [125-127], MOLT-3 human leukemic cell line [128], and in intravascular leukocytes isolated from rat renal iso- and allografts [48]. Moreover, MOLT-3 produce more ACh than other T-cell lines and express CHT1 on a higher level while ChAT activity remains similar in all cell lines [110]. This shows that high affinity choline uptake is essential for ACh synthesis in non-neuronal cells as well as in cholinergic neurons. In intravascular leukocytes from rat renal allografts, increased ACh levels correlate with higher CHT1 and ChAT expression [48].

1.4.5 ACh transport and release – vascular acetylcholine transporter (VAChT) and organic cation transporters (OCTs)

In neuronal cells, VAChT is responsible for the transport of newly synthesised ACh into synaptic vesicles (the concentration of ACh in these vesicles can be 100-fold higher than in the cytoplasm) [107, 129-130]. The VAChT gene is localised within the first intron of ChAT gene and both proteins have been co-localised in cholinergic neurons [131]. Lips *et al.* [113] showed that among non-neuronal cells, VAChT is localised in rat secretory cells of bronchial epithelium. No VAChT expression was found in skin [132], T-cells [107] or rat ciliary epithelial cells [92]. OCTs however, have been reported to be involved in ACh release in respiratory epithelium (OCT1, OCT2, OCT3) [92, 113] and human placenta (OCT1 and OCT3 [91]). Furthermore, OCT1/2 double knockout mice have an increased epithelial ACh content [133]. The presence of OCTs has been investigated in a variety of human and rodent cells and tissues. Their distribution is summarised in following table (Table 1.1):

	OCT1		OCT2		OCT3	
	h	r	h	r	h	r
small intestine	+	++	+	+	+	+
liver	++	++	-	++	++	+
spleen	+	+	+	Ø	-	+
trachea	+	+	+	+	+	+
lung	+	+	+	+	+	+
kidney	+	++	++	++	+	+
skin	+	+	+	+	+	+
blood vessels	Ø	+	Ø	-	+	+
brain	+	+	+	+	+	+
spinal cord	Ø	Ø	Ø	Ø	Ø	Ø
epithelial cells	+	+	+	+	+	+
neurons	Ø	Ø	+	+	+	+
lymphocytes	Ø	Ø	Ø	Ø	Ø	Ø
macrophages	Ø	Ø	Ø	Ø	Ø	Ø

Table 1.1: **Tissue distribution of OCTs.** ++ very strong expression, + strong expression , - no expression, Ø expression has not been investigated. h, human; r, rodent [according to [134]].

1.4.6 ACh degradation - acetylcholinesterase (AChE)/butyrylcholinesterase (BChE)

Two families of cholinesterases (ChE) are present in vertebrates: AChE and BChE [135]. In addition to neuronal cells, their expression was detected in virtually all mammalian non-neuronal cells [94, 136-138]. Within milliseconds after release, ACh is hydrolysed by AChE into choline and acetate [93-94]. Thus, the widespread action of ACh is prevented and restricted to the vicinity of cells, which are able to release this signaling molecule [93].

1.4.7 AChE/BChE inhibitor – rivastigmine

In his studies on the role of nicotine in pathological angiogenesis, Cooke *et al.* [139] showed that inhibition of AChE with neostigmine (and therefore increasing the availability of ACh) accelerates the migration of EC *in vitro*. The effect was similar to low dose VEGF, and suggested the involvement of both ACh and VEGF in angiogenesis [139]. In this study, another inhibitor – rivastigmine - has been used. Rivastigmine tartrate is a dual-specific, reversible inhibitor of both AChE and BChE [140], widely used in Alzheimer's patients for treating dementia [141].

2. Hypotheses

Chronic allograft vasculopathy (CAV) is an important aspect of chronic allograft injury (CAI), which limits the long-term success of renal transplantation. The pathogenesis of CAV is ill-defined and no effective therapies exist. Acute rejection episodes are a major risk factor for CAV. Our laboratory recently demonstrated that leukocytes, which strongly accumulate in allograft blood vessels during fatal acute rejection, produce ACh, which has the potential to provoke vascular remodelling. Here, we test the hypotheses that 1) ACh is produced by intravascular graft leukocytes during the development of renal CAV and that 2) Endogenous ACh contributes to the pathogenesis of CAV.

3. Materials and methods

3.1 Materials

3.1.1 Reagents and consumables

2-mercaptoethanol (ß-mercaptoethanol) (Sigma-Aldrich, Seelze; M-6250)
3,3'-diaminobenzidine tetrahydrochloride (Sigma-Aldrich, Seelze; D5905)
6 x loading dye solution (Fermentas, St. Leon-Rot)
Acetic acid (glacial) 100% p.a. (Merck, Darmstadt; 1.00063.1011)
Acetone p.a. (Merck, Darmstadt; 1.00014.1011)
Agarose, Ultra Pure™ (Invitrogen, Barcelona, Spain; 398611)
Aluminum potassium sulfate (Merck, Darmstadt; 1042)
Ampicilin (Ratiopharm, Ulm)
Aniline Blue, diammonium salt (Sigma-Aldrich, Seelze; 415049)
Aniline, ACS reagent ≥99.5% (Sigma-Aldrich, Seelze; 242284)
Aqua ad injectabilia (B. Braun, Melsungen; 3450317/6874361)
Aqua B. Braun (sterile water for irigation) (B. Braun, Melsungen; 75/12604052/0503)
APS, ammonium persulfate ≥98% p.a. (Roth, Karlsruhe; 9592.3)
Azokarmine G (Sigma-Aldrich, Seelze; A109-1)
Brilliant Blue G, ≥90% (TLC) (Sigma-Aldrich, Seelze; B5133)
BSA, albumin bovine fraction V (Serva, Heidelberg; 15903)
Citric acid monohydrate p.a. (Merck, Darmstadt; 1.00244.0500)
DNA ladder, GeneRuler™ 100 bp (Fermentas, St. Leon-Rot)
Dulbecco's PBS 1 x (Ca2+and Mg2+-free) (PAA Laboratories, Pasching, Austria; H15-002)
EDTA, ethylenediaminetetraacetic acid (Sigma-Aldrich, Steinheim; E9884)
EnVision® System-HRP labelled polymer anti-rabbit (Dako, Carpinteria, USA; K4003)
EnVision® labelled polymer-AP mouse/rabbit (Dako, Carpinteria, USA; K4018)
Ethanol p.a. (Sigma-Aldrich, Seelze; 322205)
Ethidium bromide solution 1% (10 mg/ml) (Roth, Karlsruhe; 2218.2)
Fast Blue BB Salt (Sigma-Aldrich, Steinheim; F3378)
Fast Red TR Salt (Sigma-Aldrich, Steinheim; F6760)
Filter paper, Whatman® (GE Healthcare Ltd., Buckinghamshire, UK)
Glycergel Mounting Medium (Dako, Carpinteria, USA; 10016653)
Glycerol for electrophoresis, ≥99% (Sigma-Aldrich, Steinheim; G8773)

Glycine ≥99% p.a. (Roth, Karlsruhe; 3908.2)

Goat-anti-rabbit immunoglobulins/HRP; polyclonal (Dako, Glostrup, Denmark; P0448)

Haematoxylin (Merck, Darmstadt; 15938)

HCl, hydrochloric acid 1 N (Merck, Darmstadt; 1.09057.1000)

HCl, hydrochloric acid ≥25% p.a. (Roth, Karlsruhe; 6331.1)

Heparin ratiopharm 25 000 IE/5 ml (ratiopharm, Ulm)

Hydrogen peroxide, H_2O_2, 30% p.a. (Merck, Darmstadt; 1.07209.1000)

IQTM SYBR® Green Supermix (Bio-Rad, München; 170-8880)

Isofluran (Forene, Abbott GmbH & Co. KG, Vienna)

Isopropanol, 2-propanol p.a. (Sigma-Aldrich, Steinheim; 33539)

KH_2PO_4, potassium dihydrogen phosphate p.a. (Merck, Darmstadt; 1.04873.0250)

Levamisole hydrochloride (Sigma Chemical, St. Louis, USA; L-9756)

Loading dye solution (6 x) (Fermentas, St. Leon-Rot)

Lumi-Light Western Blotting Substrate (Roche Diagnostics, Mannheim; 12015200001)

Methanol p.a. (Sigma-Aldrich, Steinheim; 32213)

Methenamine silver plating kit (Merck, Darmstadt; 1.00820.0001)

$MgCl_2$, 25 mM (Promega, Madison, WI, USA; A351B 20733028)

Micro BCA TM Protein Assay Kit (Thermo Sci., Rockford, USA; 23235)

Milk powder (Blotting grade) (Roth, Karlsruhe; T145.3)

M-MLV RT 5 x buffer (Promega, Madison, WI, USA; M531A 23713924)

M-MLV RT, RNase H(-) Point Mutant (Promega, Madison, WI, USA; M368B 23031114)

NaCl, sodium chloride ≥99% p.a. (Roth, Karlsruhe; 3957.1)

NaCl, sodium chloride solution 0.9% (Diaco, Naila; 43-501/A)

NaOH, sodium hydroxide solution 1 N (Merck, Darmstadt; 1.09137.1000)

Naphtol AS-MX phosphate (Sigma-Aldrich, Steinheim; N4875)

N,N-dimethylformamide, ≥99% (Sigma-Aldrich, Steinheim; D4551)

Normal rat serum (NRS) (Harlan Winkelmann, Borchen))

Oligo(dT) 15 Primer (Promega, Madison, WI, USA; C110A 27017101)

Orange G (Sigma-Aldrich, Steinheim; O3756)

Orcein (Sigma-Aldrich, Steinheim; O7380)

Ortho-phosphoric acid 85% (Sigma-Aldrich, Steinheim; 79617)

Paraformaldehyde (polyoxymethylene), 95% (Sigma-Aldrich, Steinheim; 158127)

PCR nucleotide mix (dNTP) (Promega, Madison, WI, USA; C114G 27917909)

Percoll™ (GE Healthcare Ltd., Buckinghamshire, UK; 17089101)

Pertex (mounting medium) (Medite, Burgdorf; 177320)

Phosphotungstic acid (Sigma-Aldrich, Steinheim; P4006)

Potassium chloride p.a. (Merck, Darmstadt; 1.04936.1000)

Protease, type XIV (Bacterial) (Sigma-Aldrich, Seelze; P5147)

Protease inhibitor; Complete, mini protease inhibitor cocktail tablets (Roche Diagnostics GmbH, Mannheim; 11836153001)

Protein marker, Precision Plus Protein TM dual color standards (Bio-Rad, CA, USA; 161-0374)

PVDF Transfer Membrane, Immobilon™ (Millipore; Roth, Karlsruhe)

QIAquick Gel Extraction Kit (Qiagen, Hilden; 28704)

Rabbit-anti-guinea pig immunoglobulins/HRP; polyclonal (Dako, Glostrup, Denmark; P0141)

Rabbit-anti-mouse immunoglobulins/HRP; polyclonal (Dako, Glostrup, Denmark; P0161)

Random Primers (Promega, Madison, WI, USA; C118A 26891012)

Rivastigmine (Exelon®, Novartis Pharma, Nürnberg)

RNeasy® Mini Kit (Qiagen, Hilden; 74104)

RNeasy® Lipid Tissue Mini Kit (Qiagen, Hilden; 74804)

Rotiphorese® Gel 30 (aqueous 30% acrylamide and bisacrylamide stock solution at a ratio of 37.5:1)

RNase inhibitor, rRNasin® (Promega, Madison, WI, USA; N251A 27838805)

Roti®-Histol (Roth, Karlsruhe; 6640.1)

SDS (sodium dodecyl sulfate) ultra pure ≥99% (Roth, Karlsruhe; 2326.2)

Silane, (3-aminopropyl) triethoxysilane, min 98% (Sigma-Aldrich, Seelze; A3648)

Silicone solution in isopropanol (Serva, Heidelberg; 35130)

Sodium azide ≥99% (Merck, Darmstadt; 8223350100)

Sodium dihydrogen phosphate dihydrate, extra pure (Merck, Darmstadt; 1.06345.1000)

Sodium hydroxide solution, 1 N (NaOH) (Merck, Darmstadt; 1.09137.1000)

Sodium hypochlorite solution 12% Cl (Roth, Karlsruhe; 9062.3)

Sodium iodite ≥ 99.5% (Merck, Darmstadt; 106525)

Sodium monohydrogen phosphate p.a. (Merck, Darmstadt; 1.06580.1000)

Sodium pentobarbital (Narcoren®, 160 mg/ml, Merial, Hallbergmoos)

Super-Signal® West Femto Kit (Thermo Sci., Rockford, IL, USA; 34094)

TEMED 99% p.a., Elektrophorese (Roth, Karlsruhe; 2367.3)

Trichlormethan/Chloroform, Rotipuran® ≥99,9% (Roth, Karlsruhe; 2006638)

Trizma® base, min ≥99.9% (Sigma-Aldrich, Steinheim; T1503)

Tween® 20 (for synthesis) (Merck, Darmstadt; 8.22184.0500)

X-Ray developer concentrate (Adefo-Chemie GmbH, Dietzenbach; 00009)

X-ray film, high performance chemiluminescence film, Amersham HyperfilmTM ECL (GE Healthcare Ltd., Buckinghamshire, UK)

X-Ray fixer concentrate (Adefo-Chemie GmbH, Dietzenbach; 00062)

Xylene extra pure (Merck, Darmstadt; 1.08685.2500)

3.1.2 Equipment

AlphaEase FC software 3.3.0 (Alpha Innotech Corporation, San Leandro, USA)

Balance, MXX-123 (Denver Instruments, NY, USA)

Block heater (Peqlab Biotechnologies GmbH, Erlangen)

Centrifuge, Micro 200R (Hettich Zentrifugen, Tuttlingen)

Digital camera CC12 (Soft imaging system GmbH, Münster)

Digital gel documentation system (Biozym, Hessisch Oldendorf)

iCycler iQ, real-time PCR system (Bio-Rad Laboratories Inc., München)

Microplate reader, FLUOstar OPTIMA (BMG Labtech, Offenburg)

Microscope, BX511F (Olympus, Japan)

Microtome, cool-cut HM355S (Micron GmbH, Walldorf)

Mixer Mill, MM301 (Retsch GmbH & Co. KG, Haan)

NanoDrop® 1000 (Thermo Scientific, Schwerte)

pH Meter, UB-10 (Denver Instruments, NY, USA)

Temperature Cycling System, PCR Sprint (Hybaid Ltd., Ashford Middlesex, UK)

Thermal Cycler, G-Storm GS482 (AlphaMetrix Biotech, Rödermark)

Water bath, 3042 (Köttermann, Uetze/Hänigsen)

3.1.3 Buffers and solutions

Acetic acid/alcohol

100 ml 96% ethanol and 1 ml acetic acid (glacial) were mixed.

Acidic Azocarmine G stain

0.1 g Azocarmine G was dissolved in 100 ml aqua B. Braun. This solution was heated up, shortly boiled and after cooling, filtered through filter papers (Whatman®). As a last step, 1 ml of acetic acid (glacial) was added.

Acidic Orcein stain

1 g Orcein was dissolved in 100 ml of 70% ethanol. After mixing, 1 ml of 25% HCl was added. This solution was prepared directly before use.

Alkaline phosphatase substrate solution

1 mg Fast Blue BB Salt/Fast Red TR Salt was dissolved in 1 ml naphtol AS-MX phosphate buffer with levamisole. Additionally, the Fast Blue solution was centrifuged before use.

Ammonium persulfate (APS) solution

200 mg APS were dissolved in 400 ml of deionised water (DI-water). Solution was prepared shortly before use.

Aniline alcohol

100 ml 90% ethanol was mixed with 0.1 ml of aniline.

Aniline Blue-Orange G stain

0.5 g Aniline Blue and 2 g Orange G were mixed in 100 ml DI-water. After dissolving, 8 ml acetic acid (glacial) were added. This solution and was heated up, boiled for short time and filtered through Whatman® filter paper.

BSA solution (protein standard)

50 mg of BSA was dissolved in 1 ml sample buffer I (2 x), heated for 5 min at 95°C and centrifuged for 5 min with 855 g. Afterwards, aliquots were prepared and stored at –20°C.

Citrate buffer (10 mM)

9.45 g citric acid monohydrate was dissolved in 4.39 l DI-water. pH was adjusted to 6.0 with 1 N NaOH (~112.8 ml) and DI-water was added to final volume of 5 l.

The Coomassie Blue destain

Following reagents were mixed:

- 350 ml methanol
- 24.5 ml acetic acid (glacial)
- 325.5 ml DI-water

The Coomassie Blue stain

Following compounds were mixed:

- 200 ml Coomassie Blue destain (see above)
- 50 mg Brilliant Blue G

Hemalum stain

1 g haematoxylin, 0.2 g sodium iodite and 50 g aluminum potassium sulfate were dissolved in 1 l DI-water, and left for 24 h. Next, 50 g chloral hydrate and 1 g citric acid monohydrate were added. The solution was boiled for 5 min and filtrated afterwards. Before use, the solution was diluted 1:10 in DI-water.

Loading gel buffer

6.06 g of Trizma® base was dissolved in 70 ml aqua B. Braun and the pH was set to 6.8 with 1 N HCl. 4 ml of 10% SDS solution was added and the final buffer volume was adjusted with aqua B. Braun to 1 l.

Naphtol AS-MX phosphate buffer with levamisole

2 mg naphtol AS-MX phosphate were dissolved in 200 µl N,N-dimethylformamide. 9.8 ml of 0.1 M Tris HCl (pH 8.2) and 4.8 mg of levamisole hydrochloride was added to the solution.

Paraformaldehyde (PA) 8%

50 ml DI-water was heated to 60°C. While stirring, 4 g PA and 75 µl 1 N NaOH were added.

PBS 10 x (stock solution)

The following compounds were dissolved in 900 ml DI-water:

- 80 g NaCl
- 2 g KCl
- 14.24 g Na_2HPO4
- 2 g KH_2PO_4

The pH was adjusted to 7.2 with 1 N HCl and the solution was filled up to a final volume of 1 l.

PBS 1 x (working solution)

The stock solution (10 x PBS) was diluted 1:10 in DI-water. The pH was adjusted with 1 N HCl to 7.2.

PBS/BSA/azide

In 20 ml 1 x PBS were dissolved:

- 0.2 g BSA
- 0.02 g NaN_3

The pH (7.6) was tested with indicator strips.

PBS/BSA/EDTA

100 ml PBS

27 mM EDTA

0.1% BSA

Percoll™solution

The following reagents were mixed:

- 8.8 ml aqua B. Braun
- 2.8 ml 1.5 M NaCl
- 16.4 ml Percoll™
- 60 µl 1 N HCl

Peroxidase substrate (DAB) solution

1 tablet 3,3'-diaminobenzidine tetrahydrochloride (DAB) was dissolved in 20 ml TBS. One ml aliquots of this stock solution were prepared and stored at –20°C.

Shortly before using, 10 µl of 1.2% hydrogen peroxide were added to 1 ml DAB stock solution.

Protease solution

This solution was prepared directly before using. One mg of protease powder was dissolved in 2 ml Tris-buffered saline (TBS).

Running buffer

The following compounds were dissolved in 900 ml DI-water:

- 6.08 g Trizma® base
- 28.84 g glycine
- 10 ml 10% SDS solution

The final volume was adjusted to 1 l with DI-water.

Sample buffer I (SB I) (2 x)

The following reagents were mixed:

- 1.25 ml 1M Tris-HCl buffer
- 4.6 ml 10% SDS solution
- 4.15 ml DI-water
- 1 protease inhibitor tablet

Sample buffer II (SB II) (2 x)

The following reagents were mixed:

- 1.25 ml 1M Tris-HCl buffer
- 4.6 ml 10% SDS solution
- 1.6 ml 2-mercaptoethanol
- 2.55 ml glycerol
- 1 protease inhibitor tablet

SDS stock solution (10%)

10 g SDS were dissolved in 100 ml DI-water.

Separating gel buffer

18.16 g Trizma® base were dissolved in 70 ml aqua B. Braun and the pH was set to 8.8 with 1 N HCl. 4 ml 10% SDS solution were added and the final buffer volume was adjusted with aqua B. Braun to 100 ml.

Sørensen's phosphate buffer (2 x)

The following compounds were dissolved in 500 ml DI-water:

- 3.08 g NaH2PO4
- 14.3 g Na2HPO4

TBS 1 x (working solution)

The following compounds were dissolved in 900 ml DI-water:

6.05 Trizma® base

9 g NaCl

The pH was adjusted to 7.6 with 5% HCl. The final volume was adjusted to 1l with DI-water.

Transfer buffer

Following reagents were mixed:

- 1.6 l DI-water
- 6 g Trizma® base
- 28.67 g glycine
- 10 ml 10% SDS solution
- 400 ml methanol

Tris-acetate-EDTA (TAE) 50 x (stock solution)

The following compounds were dissolved in 900 ml DI-water:

242 g Trizma® base

- 57.1 ml glacial acetic acid
- 18.6 g EDTA.

Final volume was adjusted to 1 l with DI-water.

TAE 1 x (working solution)

The stock solution (50 x TAE) was diluted 1:50 in dH_2O.

Tris-HCl buffer (0.1 M)

12.1 g Trizma® base were dissolved in 800 ml DI-water. The pH was adjusted to 8.2 with 1 N HCl. The volume was adjusted with DI-water to 1 l.

3.2 Methods

3.2.1 Transplantations

All animal experiments were performed by V. Grau and K. Petri.

3.2.1.1 Experimental animals

Male Lewis (LEW(RT11)) and Fischer 344 (F344 (RT1lvl)), specified pathogen-free rats were provided by Harlan Winkelmann (Borchen, Germany) or Elevage Janvier (Le Genest, Saint Isle, France). Animal care and animal experiments were performed following the current version of the German Law on the Protection of Animals as well as the National Institutes of Health (NIH) principles of laboratory animal care.

Transplantations were performed in LEW recipients at the age of about 2 months, weighting 250-300 g. LEW rats were used as recipients and as donors for isografts. F344 rats were used as donors for allogeneic transplantations.

3.2.1.2 Renal transplantation and treatment with rivastigmine

Kidneys were transplanted orthotopically to totally nephrectomised recipients, according to the technique described by Fabre *et al*. [142] except that the ureter was anastomosed end-to-end. Before surgery, donor (LEW or F344) and recipient (LEW) rats were anaesthetised with isofluran inhalation followed by 60 mg/kg sodium pentobarbital i.p. Additionally, donor rats obtained an injection of 1000 IU heparin per kg body weight. During surgery, rats were placed on a warming pad to keep their body temperature constant. Warm ischemic time was below 30 min. Recipient rats received a single dose of 30 µg ampicilin i.p. (Ratiopharm, Ulm, Germany). Isografts and allografts recipients were sacrificed at days 9, 42 and 6 months after transplantation, by an overdose of isofluran.

A group of allograft recipients, which were investigated for a period of 6 months, were orally treated with 0.75 mg/kg body weight rivastigmine mixed with 100 µl apple juice. Placebo was 100 µl apple juice mixed with 100 µl water. Animals were treated twice daily, from the 21st day after transplantation up to half a year after transplantation. After this time, rats were sacrificed by an overdose of isofluran. Graft recipients, which did not survive until day 4 after transplantation, were excluded from the experiment.

3.2.1.3 Renal function

Rats were weighted and placed in metabolic cages for urine collection. After 24 h, the volume of urine was measured as well as blood samples were obtained. Plasma creatinine and urea

concentration, as well as urine protein, creatinine, and urea were measured by the Laboratory of Clinical Chemistry, University Hospital Giessen and Marburg, Germany.

3.2.1.4 Perfusion of the renal vasculature

Leukocytes were isolated from the renal vasculature as described previously [49]. On days 9 and 42 post-transplantation, graft recipients were anaesthetised and heparinised and the kidneys were perfused with cold PBS containing EDTA and 0.1% BSA via the Aorta. 100 ml of perfusate were collected on ice via the Vena cava.

3.2.1.5 Purification of leukocytes

Perfusates were centrifuged for 10 min at 4°C (500 g). After removing the supernatant, cells were resuspended in 10 ml PBS/BSA/EDTA and counted. For density gradient centrifugation, this cell suspension was filled up to 50 ml with PBS. Each 25 ml of the suspension was transferred on Percoll™ (1.082 g/l) solution (two conical tubes, 14 ml each) and centrifuged for 30 min at 4°C (500 g). After centrifugation, about 20 ml of the fluid above the cell layer (interphase) could be removed. Afterwards, 1 ml of the interphase was collected. Interphases from both tubes were pooled, suspended in 50 ml PBS and centrifuged for 15 min at 4°C (500 g). After centrifugation, the supernatant was completely removed and pellet resuspended in PBS/0.1% BSA. Cells were counted, and aliquots of 5 x 10^6 cells were frozen in liquid nitrogen.

3.2.1.6 Organ fixation and embedding

Kidneys were cut in transversal slices of about 3 mm thickness. Specimens were fixed by immersion for 24 h in freshly dissolved 4% PA in 1 x Sørensen's phosphate buffer, followed by 24 h of washing in 1 x Sørensen's phosphate buffer at 4°C. On the 3rd day, pieces of the organ were immersed in 50% isopropanol for 30 min, and 3 x in 70% isopropanol for 2 h each. Next steps of embedding included placing the material once in 96% isopropanol and twice in 100% isopropanol for 1 h, each at RT. After dehydration, the material was incubated for 1 h in RT in the following solutions:

- 25% Roti®-Histol, 75% isopropanol
- 50% Roti®-Histol, 50% isopropanol
- 75% Roti®-Histol, 25% isopropanol
- 100% Roti®-Histol

Later on, each piece was immersed in liquid paraffin heated to 60°C, which was replaced after 2 h. The material was incubated in paraffin at 60°C over night.

3.2.2 Histology and immunohistochemistry

3.2.2.1 Silanising glass slides

Before using, glass slides were silanised according to the protocol indicated below, to prevent detachment of paraffin sections:

- incubation in 5% HCl over night
- washing in DI-water for 5 min
- placing in isopropanol for 5 min
- drying for 1 h at RT
- immersing for 5 min in 2% silanes in acetone
- immersing 2 x 5 min in 2% silanes in DI-water
- washing in DI-water for 5 min
- drying at ~100°C for 1 h

3.2.2.2 Preparation of sections, dewaxing and rehydration

7 µm sections were cut from the paraffin embedded material. 2 sections were placed on each silanised slide. All slides were first placed on slide warmer for about 30 min (38°C) to dry and then at ~100°C over night for better attachment of a section to the slide.

Before starting with the immunohistochemistry staining protocol, embedded material was dewaxed and rehydrated according to the protocol indicated below:

- 3 x 10 min xylene
- 2 x 3 min 100% isopropanol
- 3 min 80% isopropanol
- 3 min 70% isopropanol
- 3 min 50% isopropanol
- 3 min DI-water

3.2.2.3 Histology

3.2.2.3.1 Taenzer-Unna acidic Orcein-staining

To visualise arterial elastic membranes (internal and external elastic lamina), Orcein staining was performed. After dewaxing and rehydration, sections were immersed in freshly prepared acidic Orcein solution (3.1.3) for 30 min at RT. To wash out the stain, slides were rinsed with DI-water and placed in 100% isopropanol for 5 min to remove background staining, and thus

enhance the visibility of the stained elastic fibres. After 3 x 10 min in xylene, slides were mounted with Pertex.

3.2.2.3.2 Heidenhein AZAN staining

AZAN staining is a complex histochemical procedure which includes Azocarmine G and Aniline Blue to stain nuclei and erythrocytes red, muscle orange, and collagen in dark blue.
After dewaxing and rehydration, sections were treated according to the following protocol:

- immersion in aniline alcohol (3.1.3) for 1 min in RT
- staining in pre-warmed acidic Azocarmine G stain (3.1.3) at 56°C for 15 min
- washing with DI-water
- aniline alcohol for 1 min (removing background staining)
- acetic acid/alcohol (3.1.3) for 1 min
- washing with DI-water
- 2 h at RT in 5% phosphotungstic acid
- washing with DI-water
- Aniline Blue-Orange G stain for 2 h at RT
- washing with DI-water
- 96% ethanol for ~1 min (removing background staining)
- 3 x 10 min xylene
- mounting with Pertex

3.2.2.3.3 Gomori's methenamine silver staining

To visualise GBM and mesanglial matrix on renal sections, Gomori's methenamine silver staining was performed with the help of Methenamine silver plating kit (Merck), according to the manual provided by the manufacturer.

3.2.2.4 Immunohistochemistry

3.2.2.4.1 Single-staining

For the detection of antigens in this study, a two step immunohistochemical staining technique was used. First, primary antibodies were applied to the section. Bound primary antibodies were detected using the rabbit EnVision® System (-HRP/-AP) according to the manufacturer's recommendation.
The following antibodies were used:

Antigen	Host species	Dilution	Incubation condition
CHT1[*], synthetic peptide, aa29-40 of rat sequence	rabbit	1:8000	over night, 4°C
ChAT[*], synthetic peptide, aa 282-295 of rat 'common ChAT' sequence	rabbit	1:6000	over night, 4°C
CD68-like, ED1 [Abcam, Cambidge, UK]	mouse	1:500	2 h, RT

Tab. 3.1 Antibodies and conditions needed for immunohistochemical staining. CHT1, high affinity choline transporter; ChAT, choline acetyltransferase; RT, room temperature; [*] Thanks to the generosity of Prof. W. Kummer from Institute of Anatomy and Cell Biology; JLU Giessen.

After dewaxing and rehydrating (3.2.2.2), sections were rinsed for 3 min in TBS. Afterwards, sections were treated with 50 µl protease solution (3.1.3) for 15 min at RT, followed by 3 x washing with PBS. Endogenous peroxidase activity was inactivated by immersing the slides in 1% H_2O_2 in PBS for 30 min (6.6 ml 30% H_2O_2 added to 196.4 ml PBS). After washing in PBS (3 x 2 min), the sections were incubated for 30 min in 50 µl PBS/BSA/azide solution (3.1.3) to reduce unspecific antibody bindig.

For each section, 50 µl of antibody diluted in PBS/BSA/azide solution were used. For antibody titers, time and temperature of incubation see Tab. 3.1. On control sections, the primary antibody was omitted. After incubation, unbound antibodies were removed by rinsing the sections with PBS (3 x). Bound primary antibodies were detected using 40 µl EnVision® System. Heat inactivated normal rat serum (NRS) was added to the EnVision® solution at a concentration of 5% to block antibodies cross-reacting with rat immunoglobulins. After 30 min incubation at RT, unbound polymer was washed away from sections by rinsing them 3 x with TBS (for HRP labelled polymer) or 0.1 M Tris HCl buffer (for AP labelled polymer).

As a substrate for peroxidase, 100 µl of DAB solution (3.1.3) was used for each section. After 10 min incubation at RT, a brown end product was visible. DAB solution was washed away by rising the sections 3 x with PBS (to detoxify DAB all solution, wastes, tips, and cups used for storing DAB were washed with chloride hydrate before disposing). Selected sections were slightly counterstained with hemalum (dilution 1:10 in dH2O for 90 s).

The brown end product of DAB reaction is insoluble in organic solvents, therefore all slides were dehydrated in isopropanol (3 min in each: 50%, 70%, 80%, 2 x 100%), cleared 2 x in xylene and mounted with Pertex.

To visualise bound AP, two different substrate solutions were used: Fast Blue (blue product) or Fast Red (bright red product) (3.1.3). Each section was covered with 100 µl of substrate solution and placed in the dark for 20 min at RT. After incubation, slides were rinsed 3 x with PBS and mounted directly with warmed to 42°C Glycergel (aqueous mounting medium, as both end products are soluble in alcohol).

3.2.2.4.2 Peptide competition assay (PCA)

PCA experiments were performed to confirm the specificity of the immunohistochemical staining of polyclonal antibodies (CHT1 and ChAT). 100-200 µg of the peptide used to produce antibody were added to each ml of the dilution of the primary antibody and pre-incubated for 1 h at RT before application to the sections. During this time, a positive control dilution of antibodies (without peptide) was stored at RT.

3.2.2.4.3 Double-staining

To verify that cells, which express CHT1 and ChAT are intravascular monocytes, double-staining experiments with mouse monoclonal antibody (mAb) ED1 to a CD68–like protein were performed. The CD68-like antigen is expressed by the majority of macrophages, predominantly on the lysosomal membrane. First, primary antibodies (CHT1 or ChAT) were visualised with anti mouse/rabbit EnVision® AP (containing 5% NRS) and Fast Blue as chromogen (3.2.2.4.1). After rinsing with PBS, bound primary antibodies and EnVision®were detached from the sections by cooking for 15 min in a steamer in citrate buffer (3.1.3). After cooling down, the slides were washed in PBS 3 x 2 min, blocked once more with PBS/BSA/azide for 30 min and incubated for 2 h at RT with mAb ED1 diluted 1:500 in blocking solution. For antibody detection, anti mouse/rabbit EnVision® AP (+ 5% NRS) with Fast Red as chromogen were used. Three kinds of controls were prepared:

- omitting primary antibodies in both steps
- omitting anti-CHT1 or anti-ChAT antisera
- omitting mAb ED1

Slides were mounted as described in 3.2.2.4.1.

3.2.3 Protein biochemistry

3.2.3.1 Protein assay and sample preparation

Prior to electrophoresis, the total protein content was measured with the Micro BCA™ protein assay kit. For the protein assay, intravascular leukocytes isolated by renal perfusion

(3.2.1.5) were solubilised in SB I. Later on, the sample was heated for 5 min to 95°C and then centrifuged for 5 min with 855 g. From that solution, 10 µl were taken to estimate the protein content. After measuring the protein content, a suitable amount of SB I and II were added to the sample. Samples were aliquoted and stored at –20°C.

3.2.3.2 SDS-polyacrylamide gel electrophoresis (SDS-PAGE)

The following compounds were used to prepare separating gel:

- 1.83 ml dH2O
- 1.08 ml separating gel buffer (3.1.3)
- 1.46 ml acrylamide solution (Rotiphorese® Gel 30)
- 7.7 µl APS solution (3.1.3)
- 3 µl TEMED

The gel was poured in a gel caster. Next, a thin layer of isopropanol was added. Gel was left to polymerise in a humid chamber at 4°C over night. On the next day, the loading gel was prepared from following compounds:

- 1.35 ml dH2O
- 790 µl loading gel buffer (3.1.3)
- 652 µl acrylamide solution (Rotiphorese® Gel 30)
- 5.6 µl APS solution (3.1.3)
- 2.25 µl TEMED

After pouring the loading gel, a comb was placed on the top to create wells. The gel was left to polymerise at RT for 0.5 - 1 h. After polymerization, the comb was removed, wells were rinsed with running buffer (3.1.3) and the electrophoresis chamber was filled with running buffer. Directly before electrophoresis, the samples (3.2.3.1) were heated for 5 min to 95°C and centrifuged for 5 min at 1920 g. Ten µl of each sample (which corresponds to 8 µg protein) were pipetted in a well. To estimate the size of the separated proteins, 10 µl of a prestained protein marker (10-250 kDa) were loaded.

Electrophoresis condidtions:

- 10 min at 230 mA, 80 V
- 75 min at 230 mA, 120 V

3.2.3.3 Transfer

After separation on the gel, proteins were transferred to a polyvinylidene difluoride (PVDF) membrane to enable antigen detection. Before transfer, the gel was equilibrated in transfer buffer (3.1.3) for 5 min A PVDF membrane cut to the size of the gel was first soaked in

methanol for 1 min followed by 5 min in transfer buffer. Gel and membrane covered with filter paper were placed in a chamber filled with transfer buffer in the way that proteins from gel could migrate onto the membrane. After 90 min of transfer at 90 mA and 230 V, the membrane was taken out and air-dried at RT. The effectiveness of the transfer was checked by staining the gel with Coomasie blue stain.

3.2.3.4 Blocking and detection of antigens

The air-dried membrane was soaked in methanol for 1 min, followed by 5 min in PBS. In order to block non-specific protein binding sides, the membrane was placed in 5% milk powder (MP) in PBS for 1 h at RT. The membrane was incubated (under gentle agitation) with primary antibody diluted in 5% MP in PBS at 4°C over night. The dilution varied between different antibodies (see Tab. 3.2).

After incubation over night, the membrane was rinsed 4 x 7 min with PBS + 0.1% Tween® (TPBS), followed by incubation with an appropiate HRP-labelled secondary antibody (Tab. 3.2). In next step, the membrane was rinsed for 3 x 10 min in TPBS and additional 10 min in PBS. The membrane was covered with Lumi-Light Western blotting substrate for 5 min and the signal was detected using a X-ray film.

Antigen	**Host species**	**Dilution**	**Secondary antibody**	**Secondary antibody dilution & condiditons**
CHT1 [*]	Guinea pig	1/1500	Rabbit-anti-guinea pig Ig (HRP)	1/5000 in 2.5% MP; 90 min at RT
ChAT [*]	Rabbit	1/3000	Goat-anti-rabbit Ig (HRP)	1/5000 in 2% MP; 60 min at RT
GAPDH [Abcam, Cambidge, UK]	Mouse	1/20000	Rabbit-anti-mouse Ig (HRP)	1/5000 in 2.5% MP; 90 min at RT

Tab. 3.2 Primary antibodies: characteristics and conditions for detection. CHT1, high affinity choline transporter; ChAT, choline acetyltransferase; GAPDH, glyceraldehyde 3-phosphate dehydrogenase; Ig, immunoglobulin; HRP, horseradish peroxidase; MP, milk powder; RT, room temperature; [*] Thanks to the generosity of Prof. W. Kummer from Institute of Anatomy and Cell Biology; JLU Giessen.

3.2.3.5 Densitometrical evaluation and statistics

After scanning the blots, the bands were analysed by densitometry with the help of AlphaEase© FC software. Basing on the results, box plots and statistical analyses were made using the IBM SPSS Statistics 18 program.

3.2.4 Detection of mRNA

3.2.4.1 RNA isolation

RNA was isolated from intravascular mononuclear leukocytes from control kidneys, isografts and allografts as well as from renal tissue with the RNeasy® Mini Kit. As a positive control, total RNA was isolated from the trachea of healthy LEW rats with the RNeasy® Mini Kit and spinal cord with RNeasy® Lipid Tissue Mini Kit (Qiagen) according to the manual provided by the manufacturer. For each isolation, approximately 5 x 10^6 purified leukocytes or 30 mg tissue were used. The concentration of isolated RNA (given in µg/µl) was measured spectrophotometrically using NanoDrop® 1000. Negative controls were performed by omitting the reverse transcription step and by adding H_2O instead of the DNA template.

3.2.4.2 Synthesis of complementary DNA (cDNA)

After RNA isolation, reverse transcription was performed. To 0.5-1 µg of RNA, a mixture of random hexamers and oligo-dT primers was added at a concentration of 1 µg per 1 µg RNA. dH2O was added to a volume of 10 µl and the mixture was incubated for 5 min at 70°C and 5 min at 4°C. Next, a mastermix was prepared:

- 5 µl M-MLV RT 5 x buffer
- 1.5 µl PCR nucleotide mix (dNTP)
- 0.5 µl RNase inhibitor
- 0.5 µl M-MLV RT
- 7.5 µl dH2O

The reagents were mixed and combined with pre-incubated 10 µl of tRNA and primers. The final sample volume was 25 µl. The mixture was incubated for 10 min at 25°C, 1 h at 40°C and finally 15 min at 70°C. The obtained cDNA was ready for direct use or could be stored at –20°C.

3.2.4.3 Real-time quantitative PCR (qPCR)

qPCR was performed on an iCycler iQTM real-time PCR system (Bio-Rad), and the results were analysed with the iCycler iQTM real-time detection system software.

For preparing a master mix, the following reagents (for each sample) were used:

- 1 µl cDNA
- 10.5 µl dH_2O
- 12.5 µl IQTM SYBR® Green Supermix
- 1 µl forward and reverse primers mixture (primer list – see Tab. 3.3)

After an initial polymerase activation and denaturation step at 95°C for 8.5 min, samples went through 40 amplification cycles: 95°C for 25, 60°C for 25, 72°C for 25 s, 5 min at 72°C. At the end, a melting curve was recorded (1 min at 95°C, 1 min at 55°C and then heating slowly at 0.5°C/s to 85°C). Samples were stored at 4°C before gel electrophoresis. For each sample, a target gene and the housekeeping gene was investigated. After data calculation (Ct values), results were analysed statistically with IBM SPSS Statistics 18 software.

Primer	Sequence (5'-3')	Accession number	Product length (bp)
PBGD fwd	GGCGCAGCTACAGAGAAAGT	NM_013168	115
PBGD rev	AGCCAGGATAATGGCACTGA		
CHT1 fwd	CAAGACCAAGGAGGAAGCCAG	NM_053521	150
CHT1 rev	GCAAACATGGAACTTGCTGA		
ChAT fwd	TGGATGGTCCAGGCACAGGAGAGC	NM_001170593.1	101
ChAT rev	TGGTCACACACCACACCGCAGGT		
OCT1 fwd	TGGCCGTAAGCTCTGTCTCT	NM_012697	151
OCT1 rev	TCAAGGTATAGCCGGACACC		
OCT2 fwd	ATCACGCCTTTCCTCGTCTA	NM_031584	161
OCT2 rev	CTGCATATTCTCGGCATCCT		
OCT3 fwd	CAATGGGAAACACCTCTCGT	NM_019230	153
OCT3 rev	ATACACCACGGCACTTGTGA		
VAChT fwd	GCCACATCGTTCACTCTCTTG	NM_031663	149
VAChT rev	CGGTTCATCAAGCAACACATC		
CarAT fwd	AGAGTTTACCCAGCGTGAGG	NM_001004085	147
CarAT rev	GGCCTTAAATCGACCAGACA		

Tab. 3.3 qPCR primer list. PBGD, porphobilinogen deaminase; CHT1, high affinity choline transporter; ChAT, choline acetyltransferase; OCT1, 2, 3, organic cation transporter 1, 2, 3; VAChT, vesicular acetylcholine transporter; CarAT, carnitine acetyltransferase; fwd, forward; rev, reverse

3.2.4.3.1 Agarose gel electrophoresis

To check the size and the purity of the amplified products, agarose gel electrophoresis was performed. 100 ml of (1.5-2%) agarose solution in TAE was heated. After cooling down to 60°C, 3 µl of ethidium bromide solution were added. After cooling down, gel was placed in the running chamber filled with TAE solution. 8 µl of each sample mixed with 2 µl of a 6 x loading dye solution were pipetted per well. To estimate the size of the product, 8 µl of a DNA ladder were loaded. Electrophoresis condition: 25 min at 230 mA, 120 V.

3.2.4.3.2 DNA sequencing

The DNA sequence of the amplified PCR-products was confirmed by DNA sequencing. Individual bands were cut from the agarose gel and the DNA was extracted with the QIAquick Gel Extraction Kit according to manufacturer's manual. Sequencing was performed by Eurofins MWG Operon (Ebersberg, Germany).

4. Results

4.1 Histopathology of kidneys transplanted in the F344 to LEW rat strain combination

Experimental kidney transplantation in the F344 to LEW rat strain combination is an established model for human CAI [42-43]. Within 6 months after transplantation, allografts develop CAV, which is characterised by intimal and medial hyperplasia (Figure 4.1, A-D). On day 9 after allogeneic transplantation, when reversible acute rejection peaks, arterial thickness (including Tunica (T.) media and T. intima) increases significantly ($p \leq 0.05$) compared with day 9 isografts. However, on day 42 after transplantation, there are no significant changes between isografts and allografts, and the arterial thickness is comparable with the one of healthy control kidneys. Six months after transplantation (on day 182), significant changes ($p \leq 0.05$) in the thickness of arterial wall can be observed in allografts compared with isografts. The lumen of the arteries in allografts on day 182 is dramatically reduced compared with the arterial lumen in healthy control kidneys (Figure 4.1, D and C respectively). The thickness of the renal arteries in all isograft groups remains similar to the thickness of the arteries in healthy control kidneys (Figure 4.1, A).

Additionally to the total thickness of arterial wall, the percentage of arteries exhibiting intimal hyperplasia was estimated. Arteries in healthy control kidneys and arteries in day 9 isografts and allografts, as well as day 42 and 182 isografts show virtually no signs of intimal hyperplasia. In day 42 allografts, however, there is a significant ($p \leq 0.05$) increase in the number of arteries exhibiting intimal changes compared with day 42 isografts. At this time point, about 30% of renal allograft arteries exhibit intimal hyperplasia (Figure 4.1 B). Six months after transplantation (on day 182), the percentage of arteries with intimal hyperplasia increases to 80% ($p \leq 0.05$) in allografts compared to about 20% in isografts (Figure 4.1 B and D).

During chronic rejection, there is a significant ($p \leq 0.05$) increase in the relative thickness of T. adventitia in all allograft groups, compared to isografts (Figure 4.2, A-C). The enlarged fibrotic adventitia surrounding allograft arteries (especially on day 9) is infiltrated by leukocytes. The diameter of adventitia surrounding the arteries does not change significantly after isogeneic transplantation (on days 9, 42 and 182), compared with healthy control kidneys. In addition to vascular changes, glomerular damage (thickening of the GBM, partial sclerosis and increase in the diameter of glomeruli), TA and IF are present in allografts but not in isografts or healthy control kidneys (Figure 4.3-4.4).

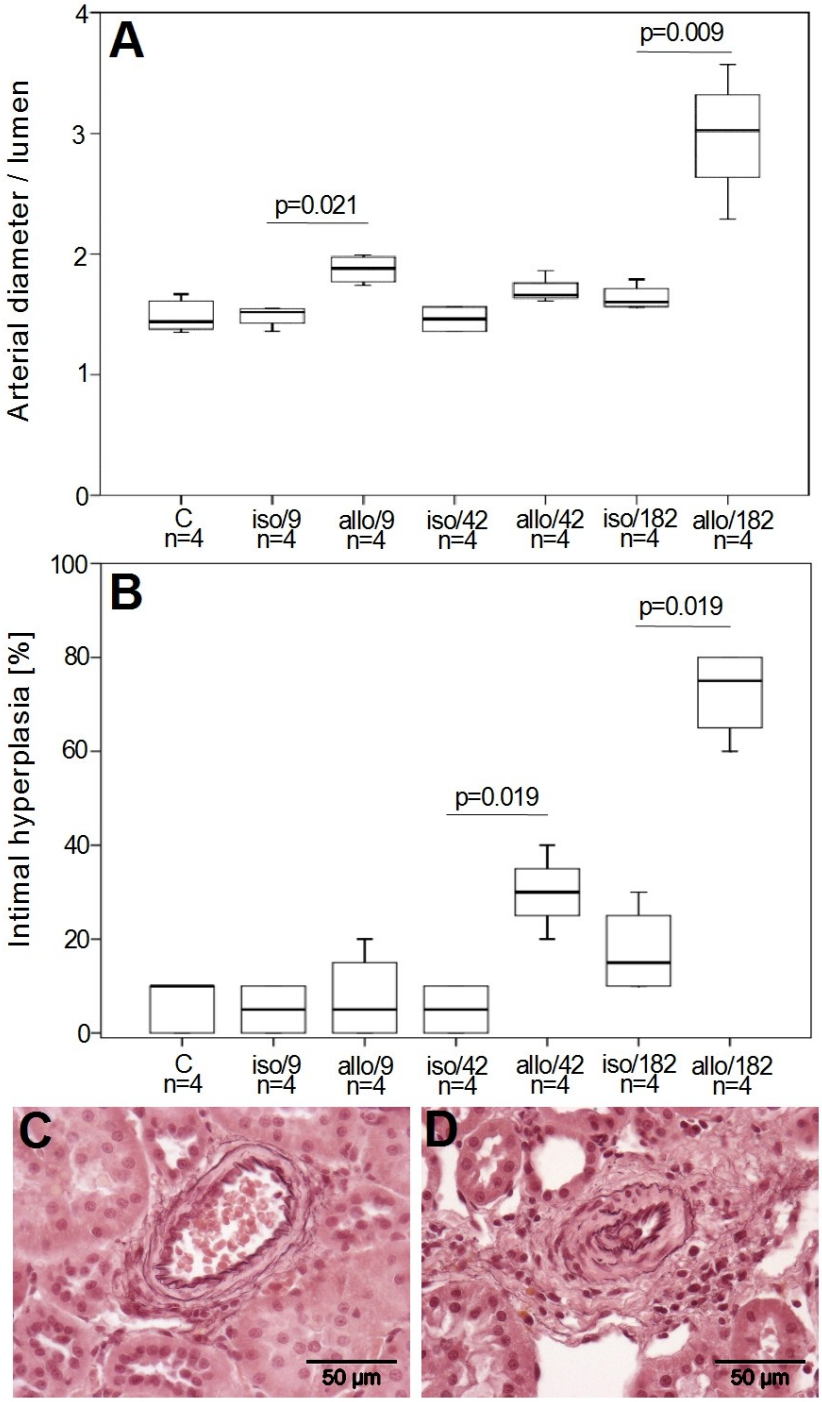

Figure 4.1: **Arterial thickness and percentage of arteries exhibiting intimal hyperplasia during chronic renal rejection.** Paraffin sections (7 µm) from the renal cortex of healthy control kidneys (C), isografts (iso) and allografts (allo) on days 9 (9), 42 (42) and 182 (182) after transplantation were stained with acidic Orcein. **A.** To measure the arterial thickness, the inner diameter of the artery surrounded by external elastic membrane (including media, intima and lumen) was divided by the diameter of the vascular lumen. **B.** The percentage of arteries exhibiting intimal hyperplasia was estimated. **C-D.** Cross-sections of an artery from a healthy control kidney and a day 182 allograft, respectively. The box plots indicate median and percentiles 0, 25, 75 and 100.

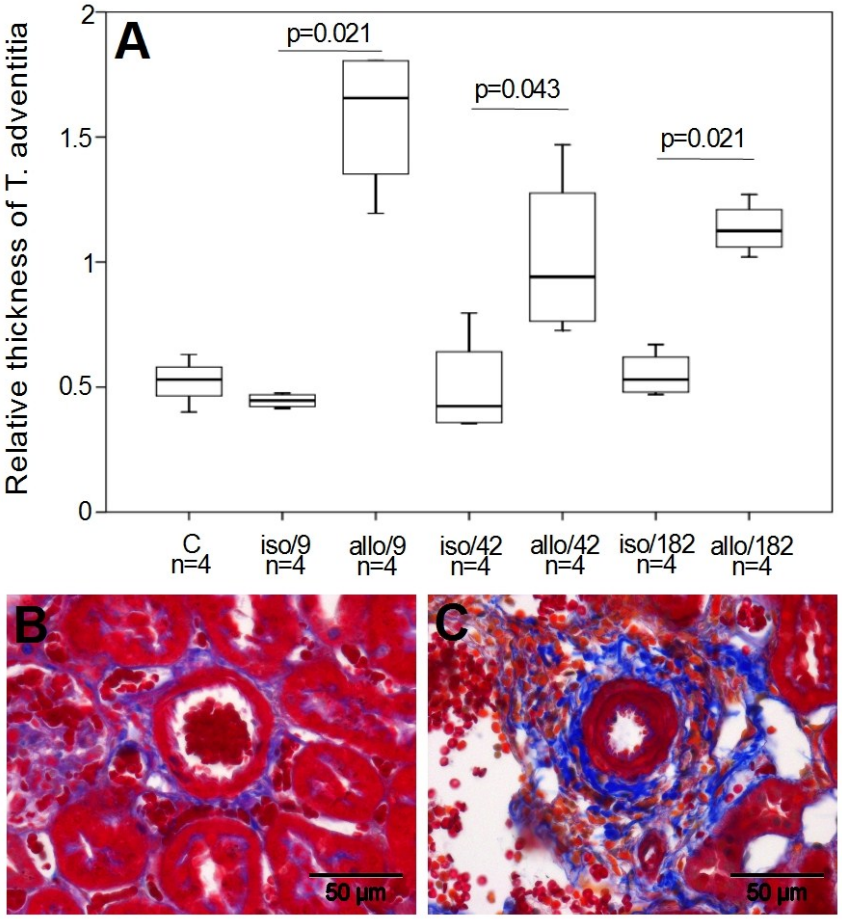

Figure 4.2: **Thickness of T. adventitia after isogeneic (iso) and allogeneic (allo) transplantation. A.** The thickness of T. adventitia was measured on AZAN stained paraffin sections from the renal cortex of healthy control kidneys (C), isografts and allografts on days 9 (9), 42 (42) and 182 (182) after transplantation. From the outer arterial diameter (including the T. adventitia, media, intima and lumen) the inner arterial diameter (including media, intima and lumen) was subtracted. This value was divided by the inner diameter. **B-C.** Azan stained cross-sections of the arteries from a healthy control kidney and a day 182 allograft respectively. The box plots indicate median and percentiles 0, 25, 75 and 100.

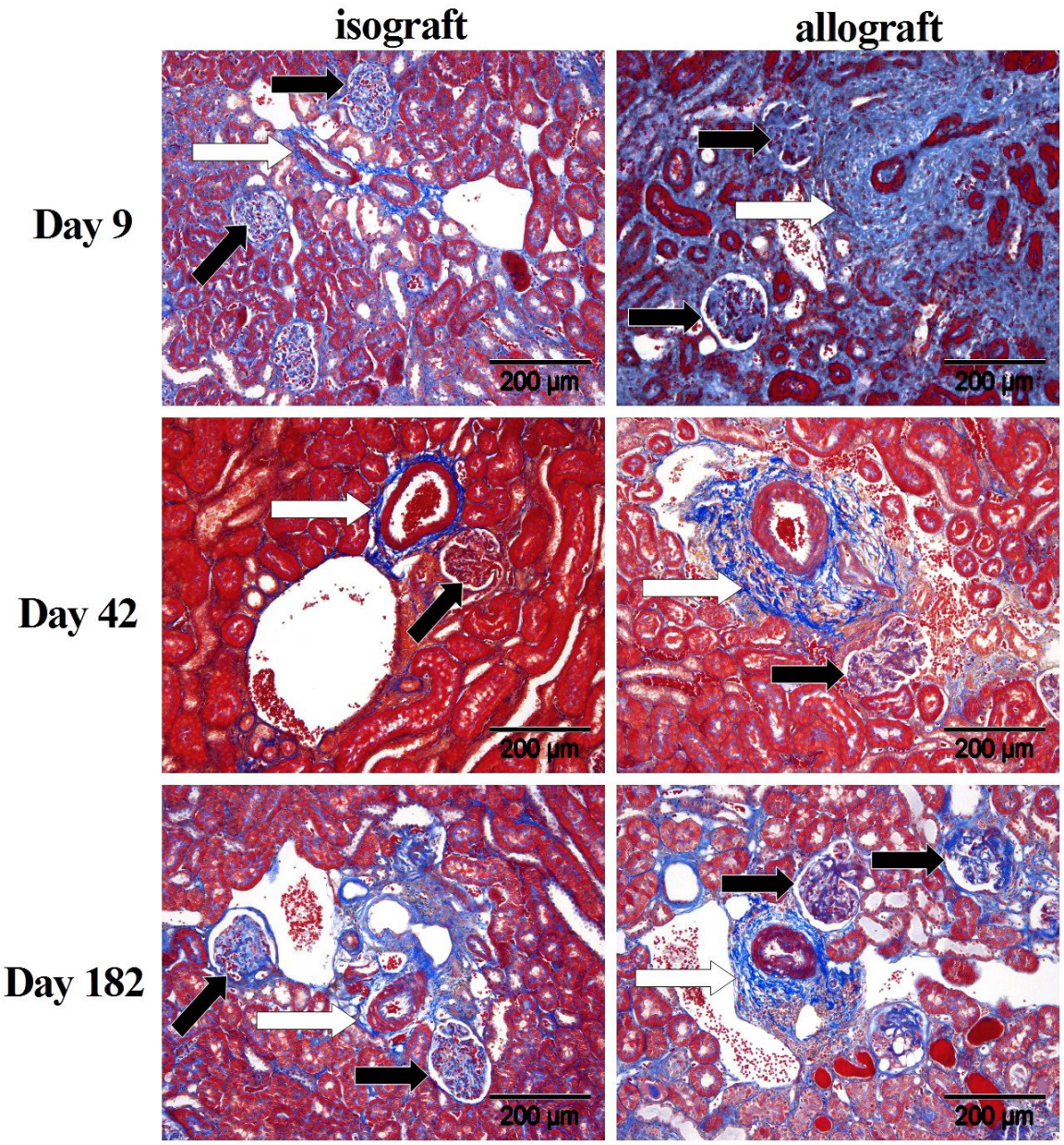

Figure 4.3: Histopathology of the renal cortex of isografts (iso) and allografts (allo) on days 9 (9), 42 (42) and 182 (182) after transplantation. Paraffin sections (7 µm) were stained with AZAN. Leukocyte infiltration, vascular remodelling, TA, glomerular damage, and general fibrosis are present in allogeneic but not in isogeneic kidneys. White arrows point to the adventitia surrounding arteries, black arrows point to glomeruli.

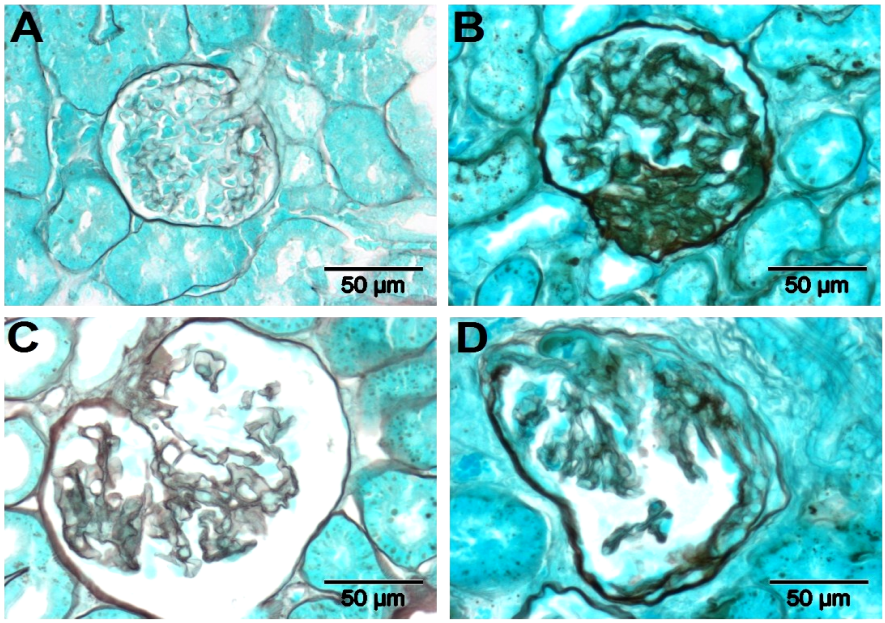

Figure 4.4: Glomerular damage during chronic renal rejection. PASM stained paraffin sections (7 µm) from the renal cortex of **A.** a healthy control kidney and **B-D.** a day 182 allograft. Thickening of the GBM, partial sclerosis and enlargement of glomeruli are visible in the allograft (B-D) but not in the healthy control kidney (A).

4.2 Number of intravascular graft leukocytes

Numerous leukocytes are seen in the vasculature of day 9 allografts (Figure 4.5). These cells are less frequent on day 42 after transplantation but still increased in comparison to isografts. The cell number remains increased in allografts until 6 months after transplantation. Leukocytes accumulate in all parts of the vascular bed including arteries of the muscular type (Figure 4.5, black arrows). Some of the leukocytes adhere to vascular endothelia or form large aggregates. To harvest leukocytes from graft blood vessels, renal transplants were intensively perfused with cold PBS/BSA/EDTA and compared with the perfusate of healthy control kidneys, which typically contain about 5 $x10^6$ leukocytes (Figure 4.6). In response to isogeneic kidney transplantation, the number of leukocytes recovered from graft blood vessels increase by about twofold at both time points investigated (Figure 4.6). Reversible rejection, which peaks around day 9, results in a dramatic increase in intravascular cells to about 135 million cells. These results corroborate data published previously [47]. The cell number drops to about 30 million cells 42 days after transplantation, which is, however, still significantly ($p \leq 0.05$) increased in comparison to day 42 isografts. Histopathological evaluation of the grafts revealed that intensive perfusion mobilised virtually all leukocytes from the blood vessels and did not disrupt the integrity of blood vessels, including the vascular endothelium (Figure 4.7).

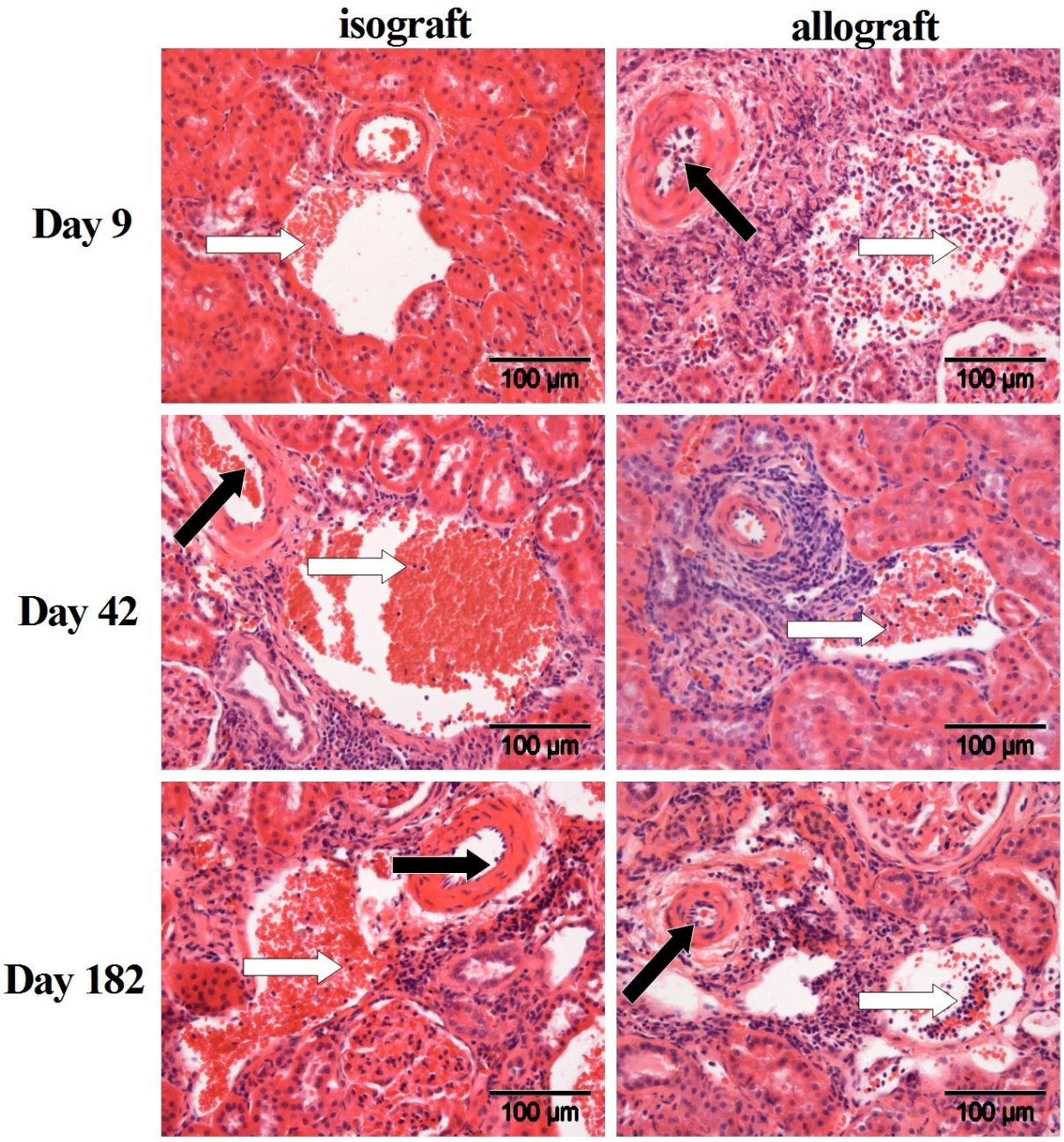

Figure 4.5: H&E staining of paraffin sections from the renal cortex of isografts and allografts on days 9, 42 and 182 after transplantation. Numerous leukocytes accumulate in the vascular bed of renal allografts on day 9 after transplantation. The number of intravascular leukocytes in renal allografts remains elevated until 6 months after transplantation. White arrows are pointing on leukocytes accumulating in the lumen of the veins and black arrows to the leukocytes present in the lumen of renal arteries.

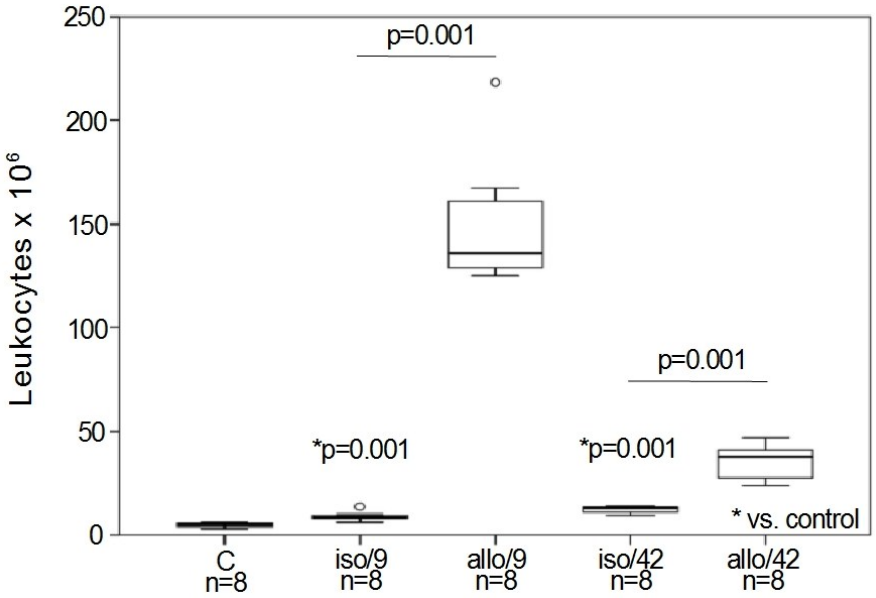

Figure 4.6: **Number of leukocytes in vascular perfusates** of untreated LEW kidneys (control, C), isografts (iso) and allografts (allo) on day 9 (9) and day 42 (42) post-transplantation. The box plot indicates median and percentiles 0, 25, 75 and 100; circles indicate data beyond 3 x standard deviation.

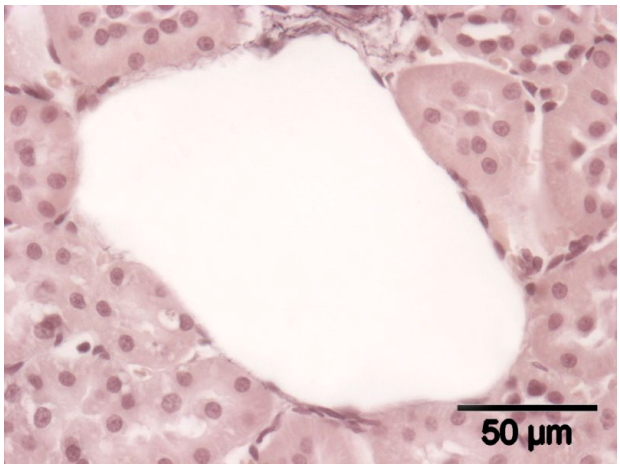

Figure 4.7: Acidic Orcein staining of paraffin section from the renal cortex of a perfused kidney.

4.3 Expression of CHT1, ChAT and CarAT mRNA by graft blood leukocytes

The mRNA-expression of CHT1, ChAT and CarAT was analysed by RT-PCR in mononuclear leukocytes isolated from renal F344 to LEW allografts, isografts and healthy control kidneys from LEW rats. Increased amounts of CHT1 mRNA were detected by real-time RT-PCR in intravascular leukocytes from day 9 and day 42 allografts in comparison to the respective isografts ($p \leq 0.05$) (Figure 4.8, A). In comparison to controls, isograft

leukocytes expressed lower amounts of CHT1 mRNA ($p \leq 0.05$). ChAT mRNA was only detected in some samples, although in addition to real-time RT-PCR, conventional and nested RT-PCRs were applied (data not shown). In the spinal cord and in the trachea, which served as positive controls, CHT1 and ChAT mRNA were detected.

In addition to ChAT mRNA, the expression of CarAT mRNA by intravascular graft leukocytes was investigated. There are no significant differences in the CarAT mRNA-expression by intravascular leukocytes isolated from isografts and allografts on day 9 compared with leukocytes from healthy control kidneys. CarAT mRNA-expression in isografts on day 42 also remains on the control level. However, there is a significant ($p \leq 0.05$) increase in mRNA-expression in allografts on day 42 compared with isografts (Figure 4.8, B). After real-time RT-PCR, the melting curves of the products (CHT1 and CarAT) indicated homogeneity and electrophoresis revealed a single band with the expected molecular weight (150 bp for CHT1 and 147 bp for CarAT). DNA sequencing confirmed the specificity of the PCR. In negative controls, no product was obtained.

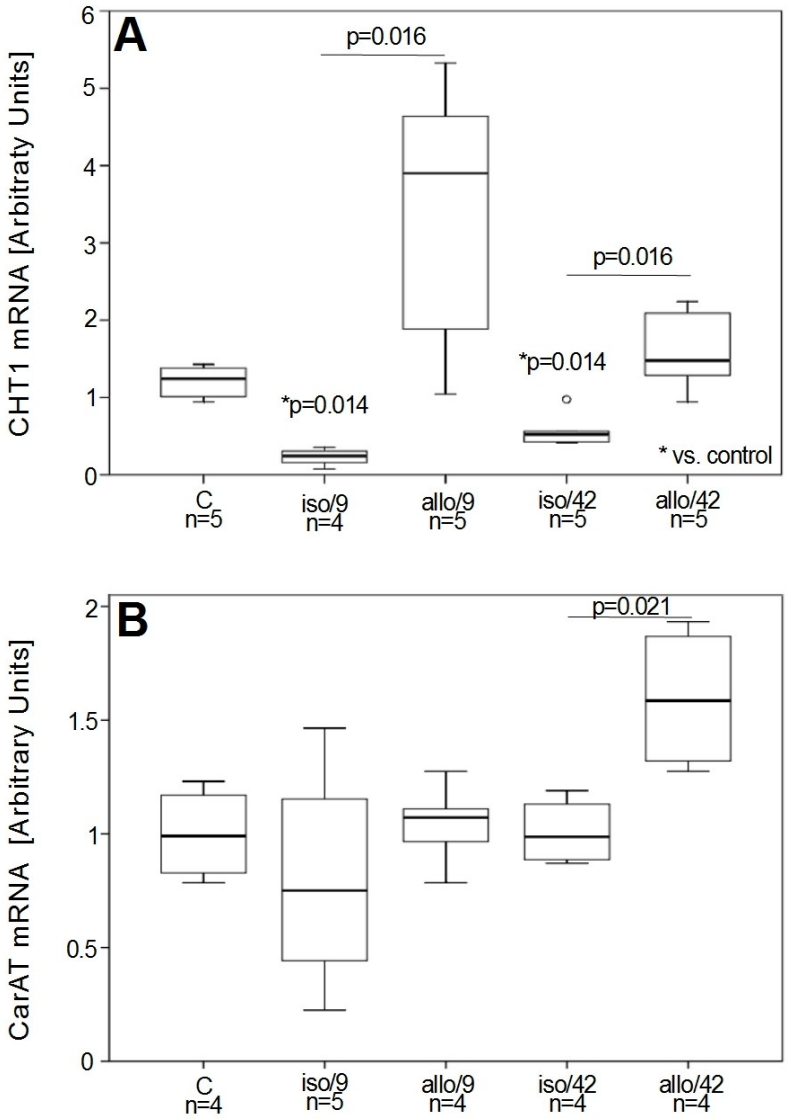

Figure 4.8: Quantitative RT-PCR analyses of A. CHT1 and B. CarAT mRNA-expression in intravascular leukocytes isolated from healthy control kidneys (C), renal isografts (iso) and allografts (allo) on days 9 (9) and 42 (42) after transplantation. Data are expressed as arbitrary units, which are normalised to one unit in controls. The box plots indicate median and percentiles 0, 25, 75 and 100; the circle indicates a value beyond 3 x standard deviation.

4.4 Expression of CHT1 and ChAT mRNA in renal tissue

The mRNA-expression of CHT1 and ChAT was also analysed in the renal tissue. Tissue homogenates from F344 to LEW allografts, isografts and healthy control kidneys from LEW rats were analysed by real-time RT-PCR. CHT1 mRNA is expressed in renal tissue at all time-points investigated. Only in day 42 allograft kidneys, the expression of CHT1 mRNA is significantly ($p \leq 0.05$) lower compared with respective isografts (Figure 4.9, A). ChAT mRNA is present in all isograft and allograft kidneys as well as in control renal tissue. There are no

significant changes between the groups of interest (Figure 4.9, B). The melting curves of the products indicated homogeneity and electrophoresis revealed a single band with the expected molecular weight corresponding to 150 bp for CHT1 and about 100 bp for ChAT. DNA sequencing confirmed the specificity of the PCR. In negative controls, no product was obtained.

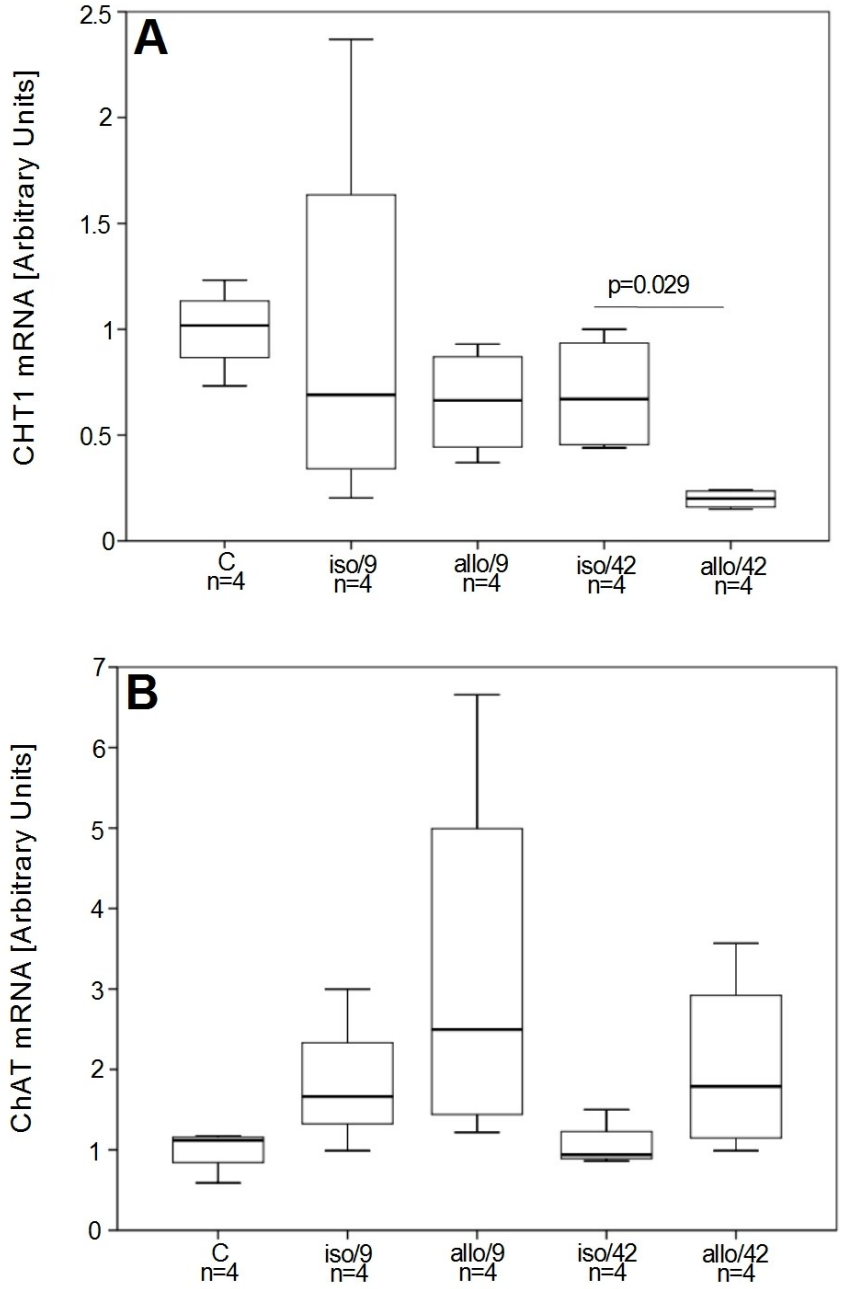

Figure 4.9: Quantitative RT-PCR analyses of A. CHT1 and B. ChAT mRNA-expression in renal tissue. Control kidneys (C), renal isografts (iso) and allografts (allo) on days 9 (9) and 42 (42) after transplantation were investigated. Data are expressed as arbitrary units, which are normalised to one unit in controls. The box plots indicate median and percentiles 0, 25, 75 and 100.

4.5 Expression of CHT1 and ChAT protein by graft blood leukocytes

CHT1 and ChAT protein expression was investigated by immunoblotting of lysates of mononuclear intravascular graft leukocytes using polyclonal antibodies against specific peptides deduced from the amino acid sequence of CHT1 and ChAT proteins [48] (Figure 4.10). Antibodies to CHT1 revealed one major band with an apparent molecular mass of 67 kDa in leukocytes from day 9 and day 42 allografts. In isografts, only a weak signal was detected. Antibodies to ChAT stained one major band with a molecular mass of about 69 kDa in leukocytes from day 9 and day 42 allografts. In isografts, the ChAT signal was weaker. Adding excess amounts of specific peptide to the primary antibody abolished CHT1 and ChAT signals (Figure 4.10). Densitometrical analyses revealed a significant increase (CHT1, p□0.05; ChAT, p□0.05) in protein expression in allografts on both day 9 and day 42 compared with isografts at the same time-points after transplantation (Figure 4.10).

4.6 Expression of CHT1 and ChAT protein by graft blood monocytes

Immunohistochemistry was performed on paraffin sections from the renal cortex of isografts and allografts (n=4 each). The immunohistochemical staining with antisera to CHT1 (Figure 4.11) and ChAT (Figure 4.12) resulted in a strong labelling of almost all leukocytes present in allograft veins. In blood vessels of isografts, the staining intensity for both proteins tended to be weaker (Figure 4.11-4.12). In addition to intravascular mononuclear leukocytes, antibodies to CHT1 and ChAT also stained endothelia, VSMC, components of the renal parenchyma, and leukocytes infiltrating allografts (Figure 4.11-4.12). To prove that most blood cells immunopositive for CHT1 and ChAT are monocytes, double-staining experiments with the antibody ED1 directed to a CD68-like antigen expressed by monocytes/macrophages [48] were performed (Figure 4.11-4.12). The specificity of the staining was verified by adding excess amounts of the specific peptides to the primary antibody solution, which dramatically reduced the staining intensity (Figure 4.11-4.12). Series of controls omitting primary or secondary antibodies were performed (Figure 4.13). They clearly show lack of unspecific straining in both single- and double-staining.

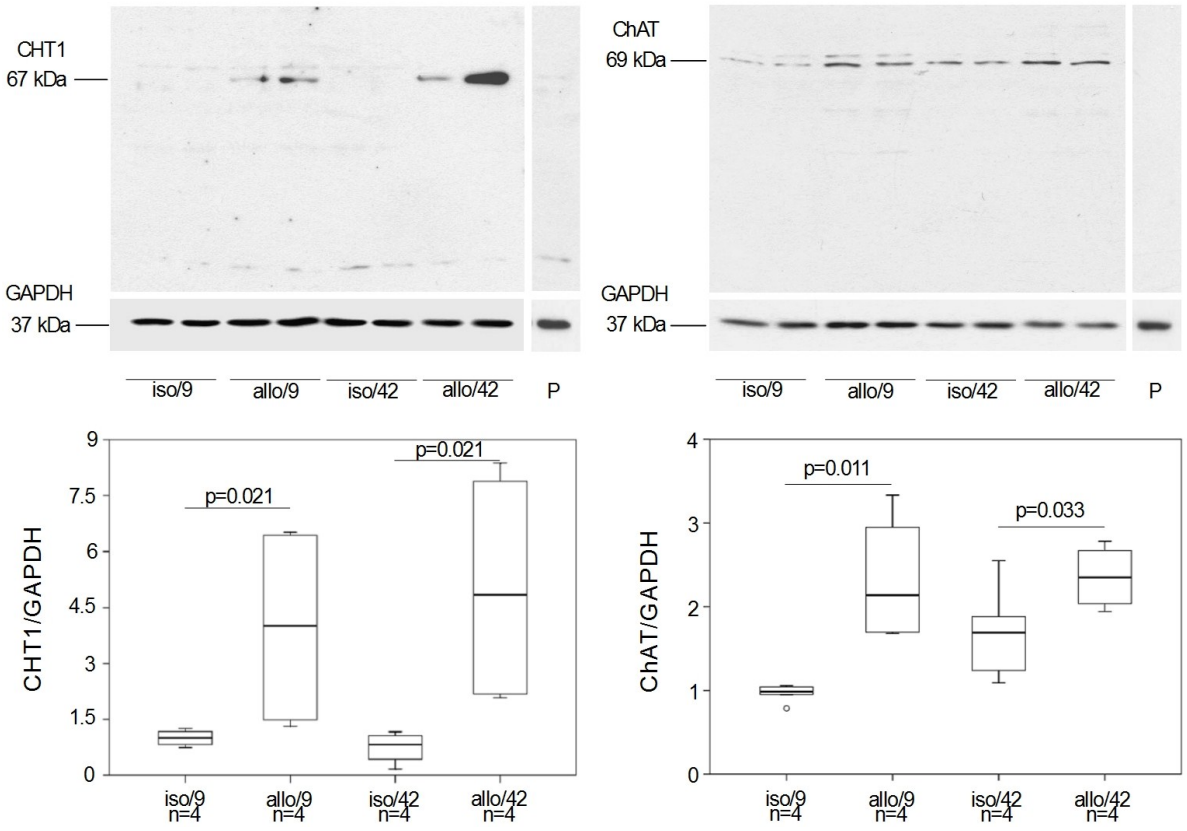

Figure 4.10: Detection of CHT1 and ChAT on immunoblots of protein extracts from mononuclear leukocytes isolated on day 9 (9) and day 42 (42) post-transplantation from the blood vessels of renal isografts (iso) and allografts (allo). To confirm equal loading, the blots were stained with antibodies to rat GAPDH. For each antibody used, one representative blot out of two is shown. The specificity of the antisera was verified by adding excess amounts of specific peptide (P) to the primary antibodies on a blot of leukocytes isolated from renal day 9 allografts. Blots were analysed densitometrically and the values obtained for CHT1 and ChAT were divided by the values for GAPDH. The mean of the data of day 9 isograft samples was set to one and all other values were calculated accordingly. Box plots show median and percentiles 0, 25, 75 and 100; the circle indicates a value below 3 x standard deviation.

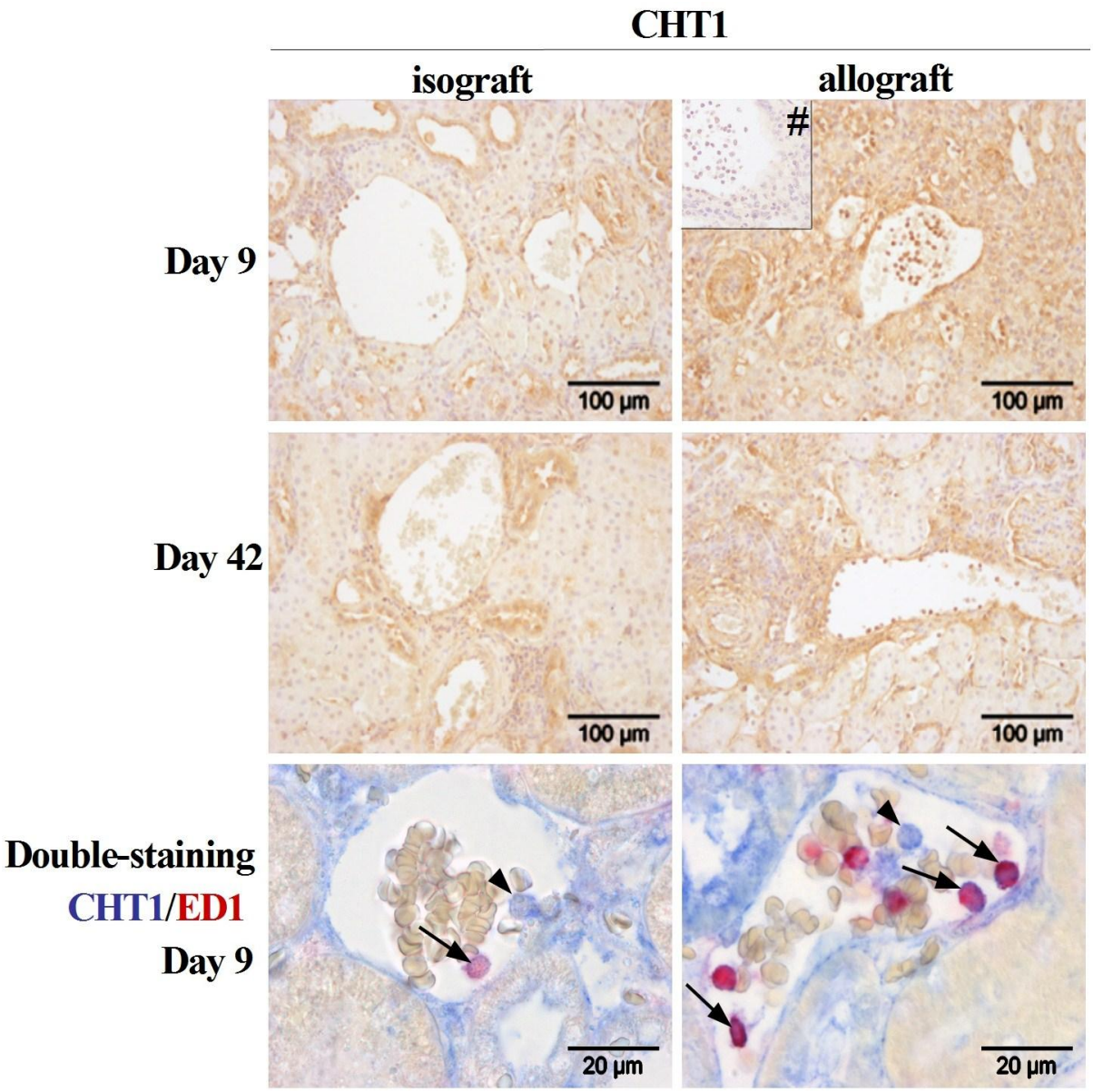

Figure 4.11: **Immunohistochemical detection of CHT1** on paraffin sections of the cortex of isogeneic (iso) and allogeneic (allo) renal transplants on days 9 and 42 after transplantation. All sections contain veins with few intravascular leukocytes in isografts and leukocyte accumulations in allografts. CHT1 was labelled in brown with a peroxidase-coupled detection system, and the sections were slightly counterstained with hemalum. The specificity of the antibody-binding was tested by adding excess amounts of the peptide used to raise the antiserum (insert in allograft day 9), which attenuated the staining intensity. Double-staining experiments using mAb ED1 directed to a CD68-like antigen indicated that monocytes exhibit CHT1 immunoreactivity. ED1 is stained in red, bound antibodies to CHT1 are stained in blue using an alkaline phosphatase-coupled detection system. The arrows are pointing to double-positive monocytes and the arrow-heads point to CHT1-immunoreactive cells negative for the CD68-like antigen.

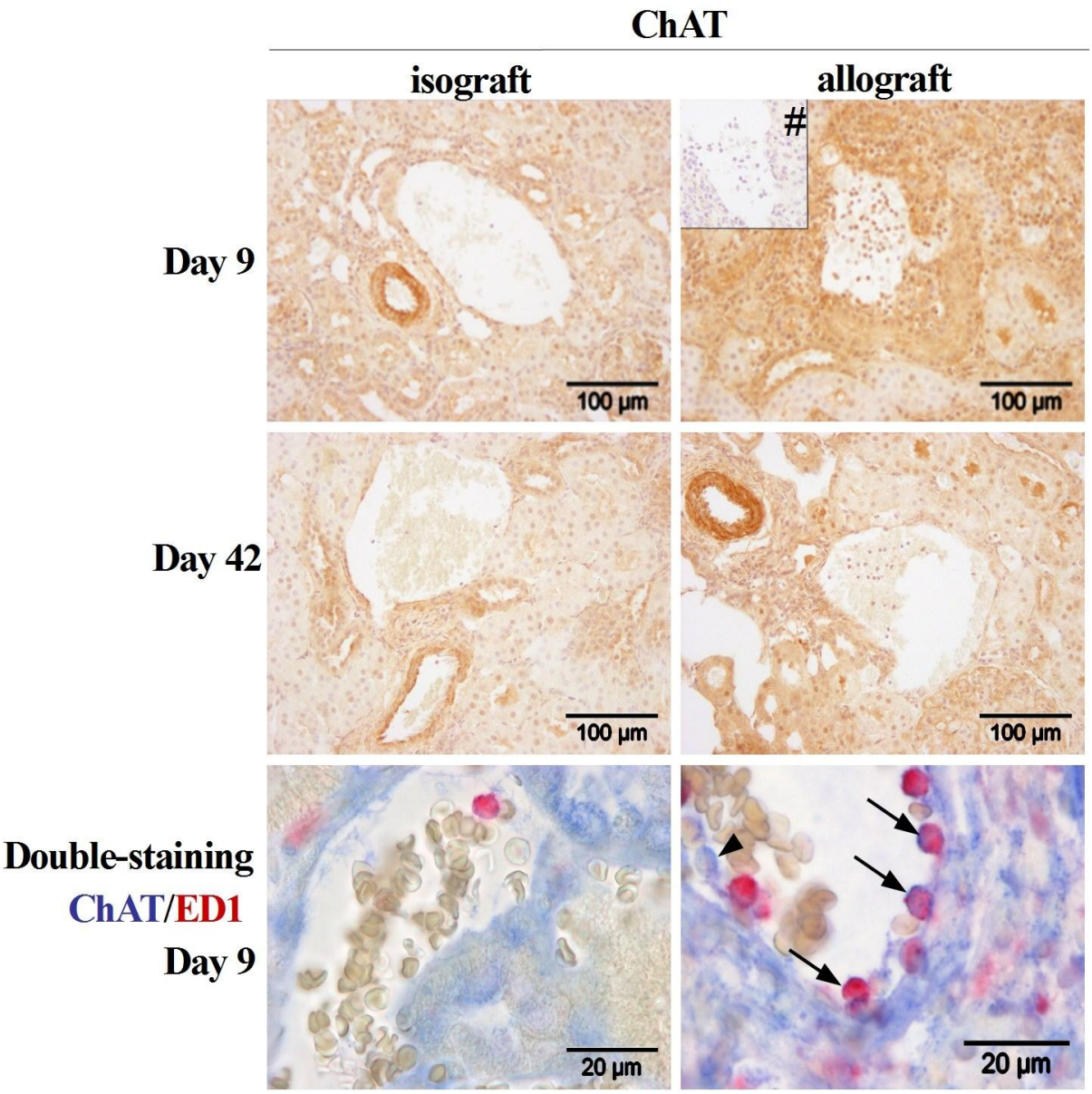

Figure 4.12: **Immunohistochemical detection of ChAT** on paraffin sections of the cortex of isogeneic (iso) and allogeneic (allo) renal transplants on days 9 and 42 after transplantation. All sections contain veins with few intravascular leukocytes in isografts and leukocyte accumulations in allografts. ChAT was labelled in brown with a peroxidase-coupled detection system, and the sections were slightly counterstained with hemalum. The specificity of the antibody-binding was tested by adding excess amounts of the peptide used to raise the antiserum (insert in allograft day 9), which attenuated the staining intensity. Double-staining experiments using mAb ED1 directed to a CD68-like antigen indicated that most cells immunopositive for ChAT are monocytes. ED1 is stained in red, bound antibodies to ChAT are stained in blue using an alkaline phosphatase-coupled detection system. The arrows are pointing to double-positive monocytes and the arrow-heads point to ChAT-immunoreactive cells, negative for the CD68-like antigen.

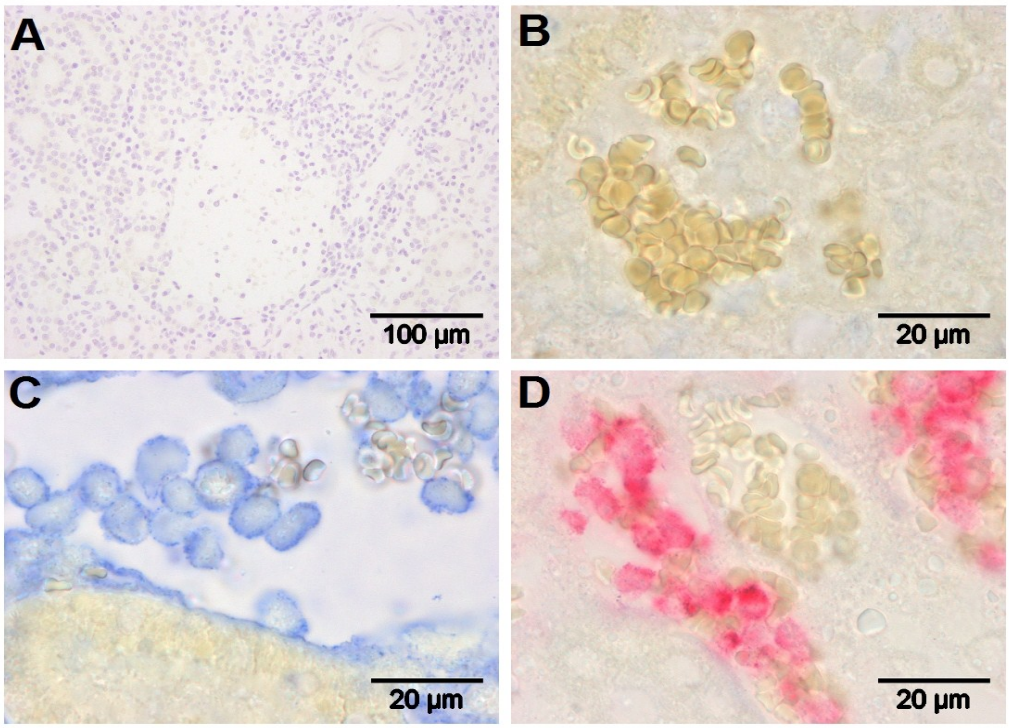

Figure 4.13: **Controls for immunohistochemical detection of CHT1 and ChAT** on paraffin sections: **A.** single-staining omitting the primary antibody; **B.** double-staining omitting both primary antibodies; **C.** double-staining omitting antibody for ED1 - only blue staining for CHT1/ChAT is present; **D.** double-staining omitting antibodies to CHT1/ChAT - only red staining for ED1 is present. The substrate for alkaline phosphatase results in a yellow to brownish unspecific back-ground, which is particularly strong in erythrocytes (**B-D**).

4.7 ACh concentration in graft blood leukocytes

To confirm ACh production, mononuclear graft leukocytes were extracted and analysed by HPLC. This experiment was performed by Prof. Dr. Ignaz Wessler from Department of Pathology, University of Mainz [143]. The chemical identity of ACh was corroborated by the use of standards and by specific degradation by ACh-esterase coupled to an HPLC column. ACh is present in all leukocyte samples isolated from grafts, but not in leukocytes from healthy control kidneys (Figure 4.14). The ACh content per million cells did not differ among leukocytes isolated from isografts and allografts, however, there is a significant ($p \leq 0.05$) increase in ACh concentration in leukocytes from day 42 isografts compared with leukocytes from healthy control kidneys (Figure 4.14).

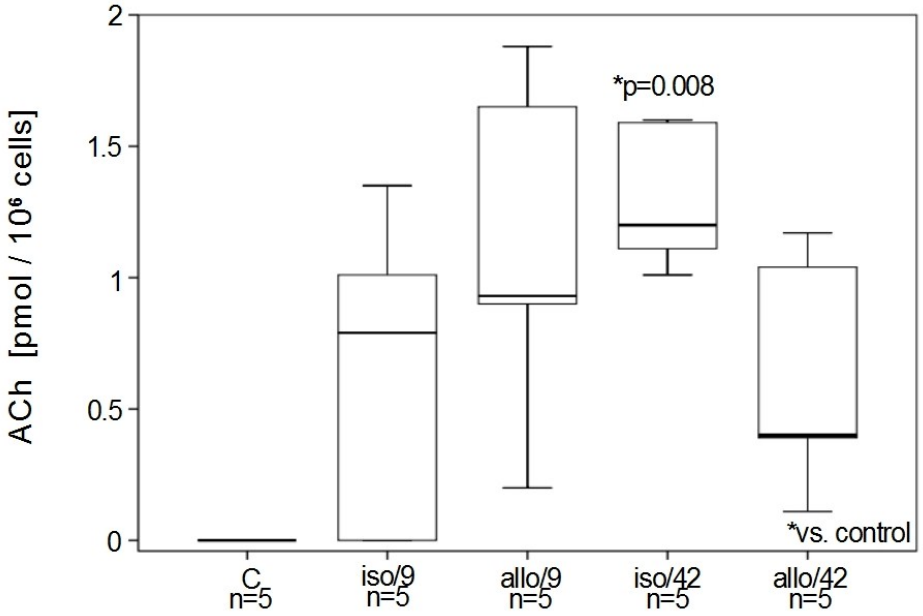

Figure 4.14: ACh concentration in intravascular leukocytes isolated from healthy control kidneys (C), isografts (iso) and allografts (allo) on days 9 (9) and 42 (42) after transplantation. ACh was analysed by HPLC combined with electrochemical detection. The box plots show median and percentiles 0, 25, 75 and 100. ACh measurements was performed by I. Wessler, Mainz.

4.8 VAChT, OCT1, OCT2 and OCT3 mRNA-expression by graft blood leukocytes

The mRNA-expression of VAChT, OCT1, OCT2 and OCT3 was analysed by real time RT-PCR in mononuclear leukocytes isolated from renal F344 to LEW allografts, isografts and healthy control kidneys. No VAChT mRNA-expression was detected. Intravascular leukocytes of all groups express OCT1, OCT2 and OCT3 mRNA (Figure 4.15). Only OCT1 and OCT2 mRNA-expression in day 9 allografts decreased significantly (OCT1, $p \leq 0.05$;

OCT2, p≤0.05) compared to isografts (Figure 4.15, A-B). OCT1 and OCT2 mRNA-expression in intravascular leukocytes from day 42 isografts and allografts remains on the control levels (Figure 4.15, A-B). OCT3 mRNA level does not differ between the groups of interest (Figure 4.15, C). The melting curves of the products (OCT1, OCT2, OCT3) indicated homogeneity and electrophoresis revealed a single band with the expected molecular weight of 150 bp for OCT1, 160 bp for OCT2, and 153 bp for OCT3. DNA sequencing confirmed the specificity of the PCRs. In negative controls, no product was obtained.

4.9 Rivastigmine-treatment of renal allograft recipients

As a proof of principle that endogenous ACh can contribute to CAV, renal allograft recipients were treated with rivastigmine, the dual-specific AChE and BChE inhibitor (n=5) or placebo (n=5). Six months after transplantation, both renal allograft groups, placebo and rivastigmine-treated animals, exhibit typical hallmarks of CAI like vascular remodelling, glomerular damage, patchy fibrosis, leukocyte infiltration or TA. The arterial thickness, including media and intima, as well as the percentage of the arteries exhibiting intimal hyperplasia is significantly (p≤0.05) increased in placebo-treated allograft recipients compared with healthy control kidneys (Figure 4.16 A-B). However, clear significant (p≤0.05) differences can be observed between rivastigmine- and placebo-treated animals (Figure 4.16, A-B). In rivastigmine-treated recipients, the proportion of arteries exhibiting intimal hyperplasia and the thickness of the arterial wall, including media and intima are increased (Figure 4.16, A-D). To exclude the possibility that rivastigmine-treatment results in arterial remodelling in other organs, arteries of recipient lungs and spleens were investigated (Figure 4.17). No differences were seen between rivastigmine and placebo-treated animals. Only lung arteries from graft recipients treated with placebo were slightly thicker compared to controls (Figure 4.17, A). To investigate graft function, creatinine clearance and proteinuria were measured monthly. During six months, renal function gradually decreased, however, there are no significant differences between placebo- and rivastigmine-treated recipients (Figure 4.18, A-B).

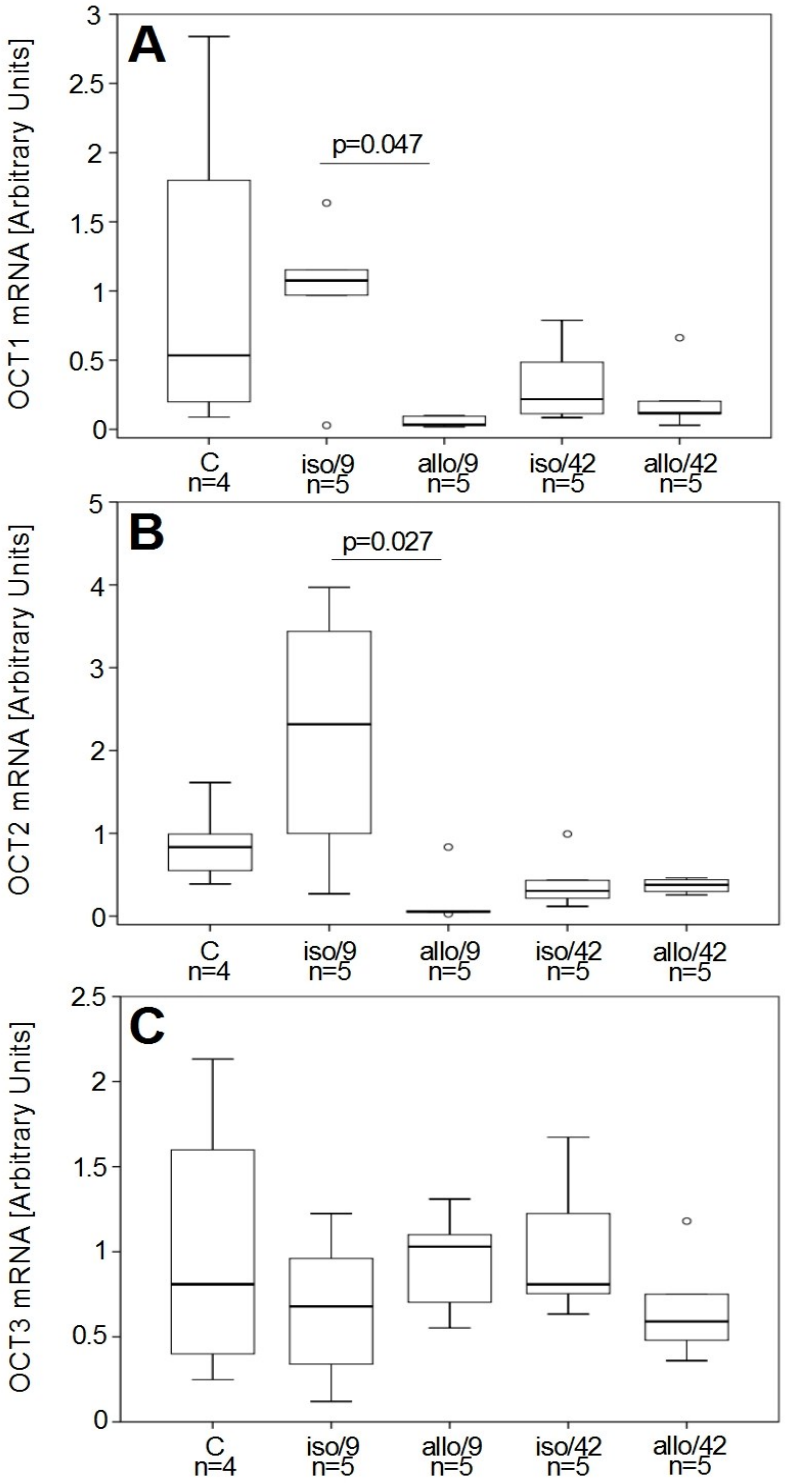

Figure 4.15: Quantitative RT-PCR analyses of (A.) OCT1, (B.) OCT2 and (C.) OCT3 mRNA-expression in intravascular leukocytes isolated from healthy control kidneys (C), renal isografts (iso) and allografts (allo) on days 9 (9) and 42 (42) after transplantation. Data are expressed as arbitrary units which are normalised to one unit in controls. The box plots indicate median and percentiles 0, 25, 75 and 100; circles indicate data beyond 3 x standard deviation.

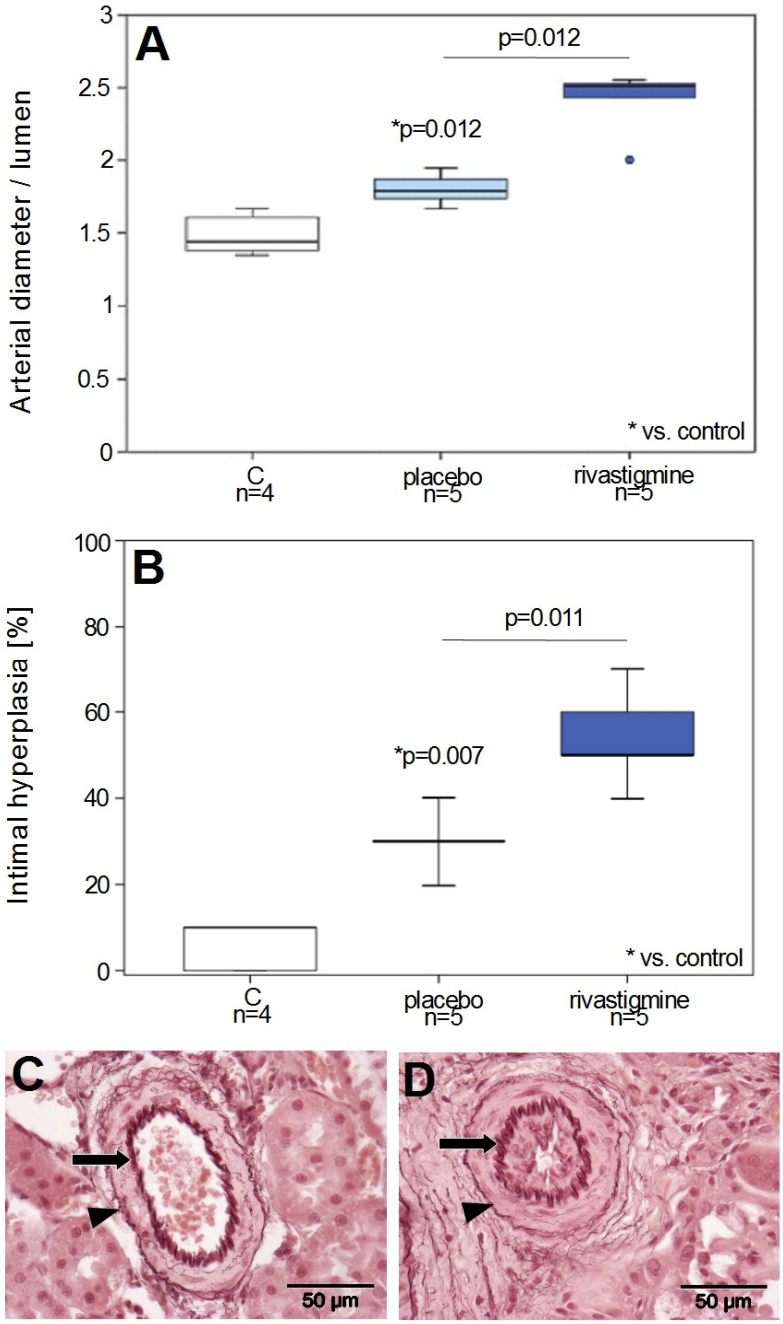

Figure 4.16: Vascular remodelling in renal allografts 6 months after transplantation from recipients treated with placebo or the cholinesterase inhibitor rivastigmine. Histological sections were stained with acidic Orcein to visualise the internal (arrow) and external (arrow-head) elastic lamina of arteries of the muscular type (**C,D**). **A.** To measure the relative arterial thickness, the inner diameter of arterial structures surrounded by the external elastic lamina, including T. media, T. intima and lumen was divided by the diameter of the vascular lumen. **B.** The percentage of graft arteries with intimal hyperplasia was determined. **C-D.** Sections of kidneys are shown depicting an example of a normal artery (control, **C.**) and **D.** an example of a severely remodelled artery (rivastigmine). The box plots show median and percentiles 0, 25, 75 and 100; the circle indicates a value below 3 x standard deviation.

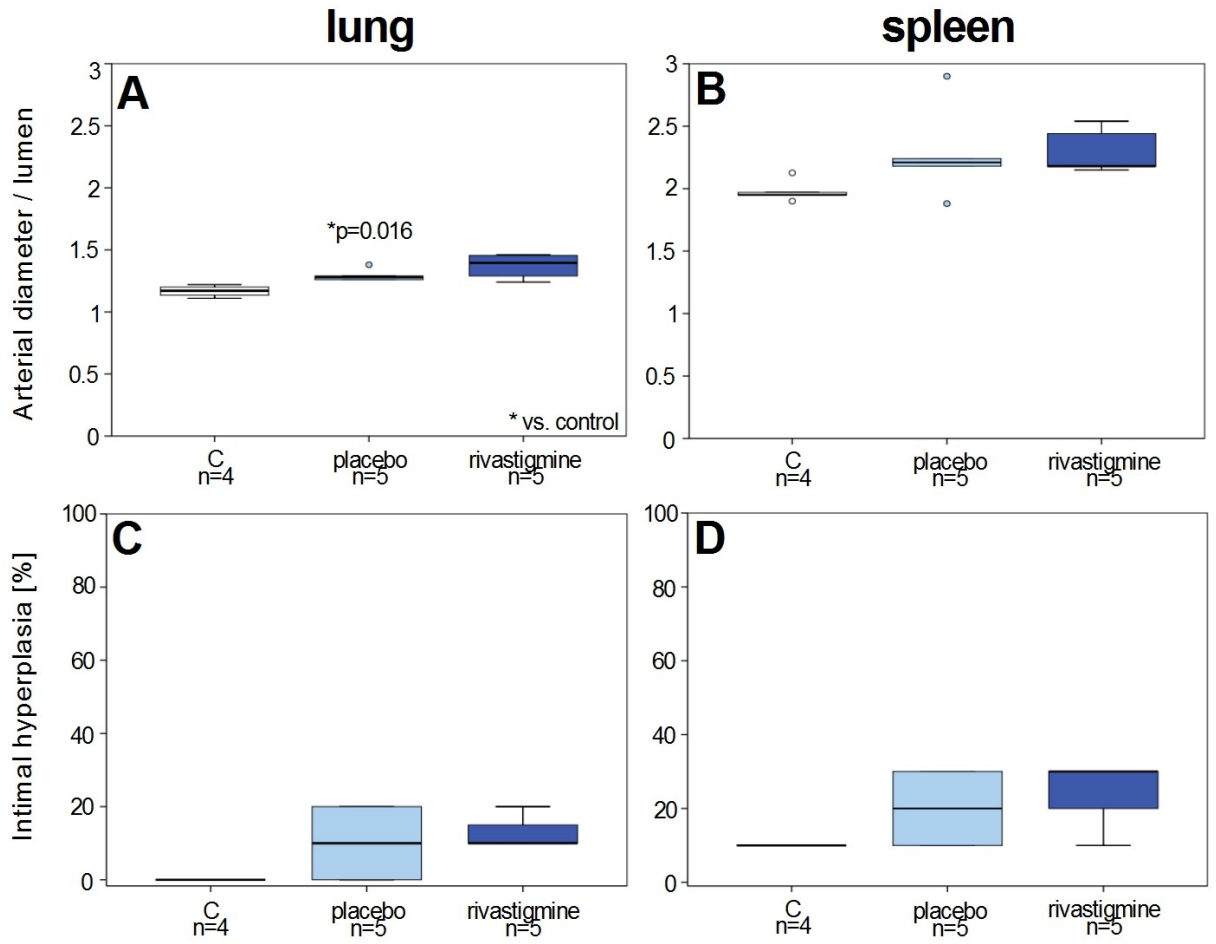

Figure 4.17: Systemic effects of rivastigmine-treatment. The vascular morphology was investigated in lungs (**A, C**) and spleens (**B, D**) of allograft recipients. Normal healthy organs from untreated rats were included as additional controls. **A-B.** To measure the relative arterial thickness, the inner diameter of arterial structures surrounded by the external elastic lamina, including T. media, T. intima and lumen was divided by the diameter of the vascular lumen. **C-D.** The percentage of graft arteries with intimal hyperplasia was determined. The box plots show median and percentiles 0, 25, 75 and 100; circles indicate data beyond 3 x standard deviation.

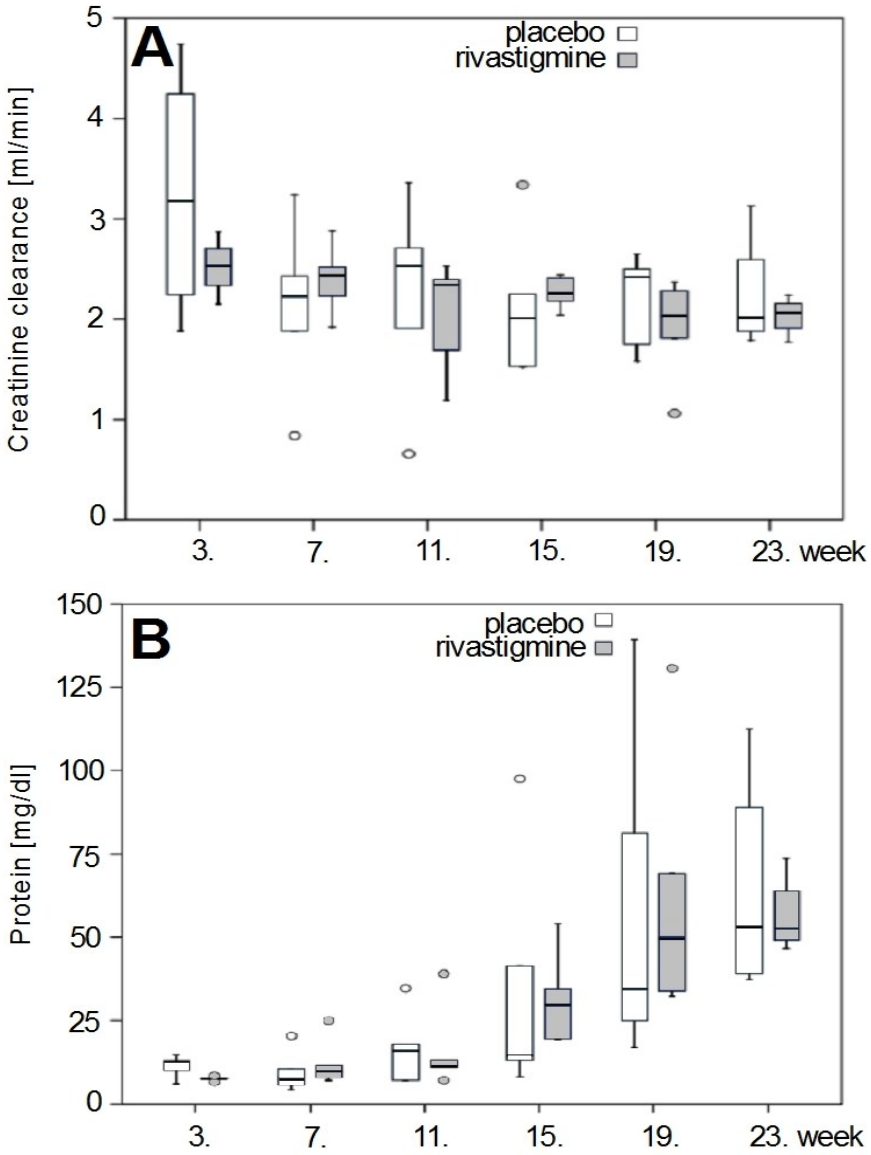

Figure 4.18: Graft function. A. Creatinine clearance and **B.** total urine protein were determined monthly for placebo- and rivastigmine-treated animals. The box plots show median and percentiles 0, 25, 75 and 100; circles indicate data beyond 3 x standard deviation.

5. Discussion

5.1 Experimental renal transplantation

Renal transplantation in the F344 to LEW rat strain combination is an established model for human CAI. It has been first described in 1969 by White *et al.* [44], followed by Mahabir *et al*. [144] one year later. Allografts pass through an acute rejection episode, which is in most studies suppressed with the calcineurin inhibitor CsA for 10 days after transplantation. In the long-run, allografts develop CAN, which is characterised by progressive proteinuria and renal dysfunction caused by histopathological lesions like glomerulosclerosis, IF/TA, mononuclear cell infiltration, and vascular remodelling [42, 145]. Numerous immunological and non-immunological factors contribute to the development of CAI. Treatment with CsA has been reported to be an important non-immunological cause [146].

CsA was first used in patients after renal transplantation and was immediately reported to have nephrotoxic properties when used at the dose based on previous animal experiments [147]. Thereafter, a lower dose of CsA was used in clinical studies, which effectively diminished the risk of acute allograft rejection [148]. Acute CsA nephrotoxicity caused functional changes in renal grafts, such as impaired tubular function, proteinuria, and reduced glomerular filtration rate. These changes were reported to be reversible after termination of the treatment [148-150]. In 1984, Myers *et al.* [151] investigated the long-term effects of CsA: the expected reversible decrease in glomerular filtration rate, irreversible progressive glomerulosclerosis and tubulointerstitial injury [151]. Later on, the chronic nephrotoxicity of CsA was confirmed [152-153]. Conflicting results were obtained in experimental kidney transplantation. In renal DA to LEW allografts, even high CsA doses did not provoke any histopathological or biochemical changes [154]. In contrast, in LEW recipients of F344 renal allografts, CsA was nephrotoxic [155].

In this project, renal transplantation was performed in the F344 to LEW rat strain combination, however, no immunosuppression was used to avoid nephrotoxicity induced by CsA. After transplantation and reversible acute rejection, allografts are spontaneously accepted. In the long-run, CAI develops with all characteristic histopathological lesions and progressive loss of function [156]. Depending on the severity of the ischemia/reperfusion injury and on the reduction of renal mass, CAI can also be seen in renal isografts [156-158]. Similar results of renal transplantation in F344 to LEW rat strain combination without CsA-treatment have been published [47, 159-161]. There are clear advantages in investigating the development of CAI in an animal model in the absence of immunosuppression. There is no

interference with acute rejection, which is an important risk factor for the development of CAN [7-9], thus, it enables to investigate factors triggering CAAN during acute rejection episodes. These factors could be promising targets for new therapeutic approaches preventing CAN. Furthermore, CAN can be investigated in the absence of potentially confounding nephrotoxic effects of CsA.

5.2 Leukocyte accumulation

In previous studies, our laboratory demonstrated that during fatal and reversible acute rejection, stunning amounts of mononuclear leukocytes accumulate in all parts of the vascular bed of the graft including arteries [47, 49]. Interestingly, the number of leukocytes present in the blood vessels of isograft recipients on days 4 [49], 9 [47], and 42 after transplantation is doubled throughout in comparison to untreated control kidneys. It is unknown if this is due to ischemia/reperfusion injury, to renal denervation or to hyperperfusion in the absence of a contralateral kidney. Pilot experiments on the time course of intravascular leukocyte accumulations in the F344 to LEW model already suggested that after reversion of acute rejection, the number of intravascular leukocytes remains at an elevated level [156]. Here, these preliminary data are corroborated. Six weeks after transplantation, the cell number in allografts increase about 3-fold compared to isografts, thus, the accumulation of intravascular leukocytes in the vascular bed of allografts is a long-lasting process.

5.3 Thickness of arterial wall during reversible acute rejection

On day 9 after allogeneic but not isogeneic transplantation, a transient increase of the relative thickness of the arterial wall including media, intima and adventitia is observed. There is, however, virtually no intimal hyperplasia, and the internal elastic membrane is intact. Previously, the adventitia was described as an element of the artery only having a supportive role. Strong evidence suggests that it actively participates in vasoconstriction and vasorelaxation [162-163]. On day 9 after allogeneic transplantation, the adventitia is infiltrated by numerous leukocytes. These cells may induce adventitial fibrosis. Later on, the number of cells surrounding the artery decreases together with the thickness of adventitia. Several factors contribute to the regulation of the vasotonus, such as NO – a vasorelaxant, and endothelin (ET-1) – a vasoconstrictive mediator. Besides being a vasorelaxant, NO regulates leukocyte adhesion and proliferation of SMC. Both NO and ET-1 are produced by EC and inflammatory cells. Impaired regulation of the vasotonus can be related with EC dysfunction, which is frequently present after allogeneic transplantation [164]. It may be related to IR

injury or damage of EC by intravascular leukocytes accumulating during reversible acute rejection [164]. ET-1 is known to be upregulated shortly after transplantation in response to IR injury [165]. Additionally, the adventitia has been shown to contract in response to ET-1, contributing to vasoconstriction [163]. Thickening of media and intima observed on day 9 after allograft transplantation is probably at least in part caused by functional changes resulting in contraction.

5.4 CAN

Within 6 months after transplantation, allograft recipients develop typical hallmarks of CAN. Vascular remodelling, including intimal and medial hyperplasia and disruption or doubling of the internal elastic membrane, is clearly visible in allograft arteries on day 182 after transplantation and increased compared with isografts. Even a small decrease in the arterial lumen caused by intimal thickening can impair renal perfusion due to the increase in the resistance of the blood flow [166]. Vascular remodelling and progressive fibrosis are not the only signs of CAI in renal allografts. Glomerular damage and TA are also present. Due to the changes in the renal tissue, the function of renal allografts is decreased compared with isografts [156].

5.5 ACh synthesis

I sought to analyse the expression of essential elements of the machinery for ACh synthesis, CHT1, ChAT and CarAT in intravascular leukocytes from renal isografts, allografts and healthy control kidneys. The results of the real-time RT-PCR show that CHT1 expression is upregulated. Unexpectedly, leukocytes from healthy control kidneys expressed higher amounts of CHT1 mRNA compared to isografts, which is in contrast to our HPLC experiments, where no ACh was detected in control leukocytes. In contrast to CHT1, ChAT mRNA was not detectable in some samples. Previously, ChAT mRNA was detected by the highly sensitive nested RT-PCR in leukocytes from the blood vessels of renal allografts undergoing fatal acute rejection [48]. As it was possible to detect small amounts of ChAT mRNA in few samples (data not shown), I assume that low levels of ChAT mRNA are also expressed by the leukocytes in other groups.

In addition to ChAT mRNA, CarAT mRNA-expression was investigated in intravascular leukocytes. CarAT has been reported to be an effective enzyme for ACh synthesis in the absence of ChAT [113, 167]. Intravascular leukocytes from all experimental groups are expressing CarAT mRNA and its level is increased in allografts on day 42 compared with all

other groups. This result is in line with the CHT1 mRNA-expression levels, which are also increased in allograft leukocytes and suggest that intravascular leukocytes produce higher amounts of ACh on day 42 after allogeneic transplantation. The results clearly show that intravascular leukocytes express the mRNA of enzymes necessary for ACh synthesis and that the mRNA-expression is increased after allograft transplantation.

On the protein level, CHT1 and ChAT were detected in intravascular allograft leukocytes both by immunoblotting and by immunohistochemistry, also suggesting that intravascular leukocytes including monocytes can produce ACh. In line with our hypothesis, both proteins were expressed at higher levels in allografts.

In addition to intravascular leukocytes, mRNA-expression of CHT1 and ChAT was analysed in homogenates of the renal tissue. CHT1 and ChAT mRNA is detected in the kidney of animals from all experimental groups, but there is no significant increase in mRNA-expression in allografts. Unexpectedly, there is a significant decrease in CHT1 mRNA-expression in kidneys of allograft recipients on day 42. As CHT1 is produced by endothelial cells, VSMC and elements of renal parenchyma [48, 125-126], damage of renal tissue due to progression of allograft rejection could be the cause of reduced CHT1 expression. However, no such effect was visible for ChAT, which is also produced by these cells. The tissue protein expression of ChAT and CHT1 was not investigated by Western blotting because this study focused on intravascular cells. There is, however, no drastic decrease in the intensity of immunohistochemical staining with antibodies to CHT1 and ChAT on sections from allografts on day 42 compared with other groups.

Recently, a new member of choline transporter family has been investigated, choline transporter-like protein (CTL-1) and has been shown to be an efficient choline transporter in rat tubular epithelial cells in the absence of CHT1 [168]. In this study, CTL-1 expression was not investigated, which may be of interest in further studies.

5.6 Leukocytic ACh content

ACh is a well-known neurotransmitter in vertebrates and invertebrates. It is also present in invertebrates without a nervous system such as sponges, where it acts as a local mediator [169]. ACh is also present in plants, fungi and in bacteria, where it plays different roles, such as the regulation of differentiation and communication [169-170]. These data show that ACh is present ubiquitously throughout the evolution and that it may regulate physiological functions as a local mediator as well as a neurotransmitter.

The detection of leukocytic ACh in intravascular leukocytes, which was evidenced by HPLC,

just indicates that ACh is produced. By this method it is, however, not possible to indicate how many ACh is actually released by intravascular graft leukocytes *in vivo*. Due to the ubiquitous expression of ACh-esterases, a reliable measurement of ACh in bodily fluids is difficult. From functional analyses *in vitro*, however, it is known that monocytes from allografts undergoing fatal acute rejection but not cells from isografts release ACh, which binds to their AChR in an autocrine or paracrine fashion [48]. As intravascular leukocytes and allograft endothelia are in direct contact to each other and allograft blood vessels are almost obstructed by leukocytes [47, 156], the velocity of the blood stream is likely to be severely impaired in allografts. Hence, we conclude that ACh released by intravascular allograft leukocytes may be locally active and bind to AChR expressed by endothelial cells.

5.7 ACh release

After proving that intravascular leukocytes produce ACh, molecules involved in the release of ACh were investigated. No VAChT mRNA- was detected in intravascular leukocytes (data not shown). In 2001, Wessler *et al.* [171-172] showed evidence that in the absence of VAChT, ACh can be released via OCT1 and OCT3 in the human placenta. In *Xenopus* oocytes, the release of ACh is mediated by OCT1 and OCT2 but not by OCT3 [173]. Similar results were shown for airway epithelial cells and urothelium [92, 113]. Additionally, OCT2 has been shown to partake in ACh transport in both directions (uptake and release) [174]. There is also evidence that the level of ACh in tracheal epithelial cells is increased in OCT1/2 double-knockout mice, due to impaired ACh release [133]. Basing on these results, mRNA-expression of all three types of OCTs was investigated. Intravascular leukocytes from all experimental groups express OCT1, OCT2 and OCT3 mRNA. According to the publications of Lips *et al.* [92, 113] it can be expected that OCT1 and OCT2 represent a major release system for ACh in intravascular leukocytes. The mRNA-expression level of these two transporters decreases upon inflammation, starting in allografts on day 9, but not in isografts and remains on a low level until day 42 in both isografts and allografts. The OCT3 mRNA-expression remains on similar levels in all groups of interest. Similar down-regulation of OCT1 and OCT2 but not of OCT3 has been shown by Lips *et al.* [175] in rat and mouse models of acute allergic airway inflammation. Although the expression of the OCTs in intravascular leukocytes was not confirmed on protein level, mRNA-expression data suggest that the release of ACh from intravascular graft leukocytes might be impaired in allografts during chronic renal rejection. Combined with the increased expression of CHT1 mRNA and CHT1 and ChAT proteins in both allograft groups, an increased level of ACh in intravascular

leukocytes isolated from allografts can be expected. However, the ACh levels are similar in intravascular leukocytes from allografts, isografts and from healthy control kidneys, which suggests the presence of additional ACh release mechanisms. Schlereth *et al.* [176] has shown that the release of ACh from human skin does not fully depend on OCTs.

5.8 ACh and CAV

To prove that endogenous ACh can promote CAV, allograft recipients were treated with rivastigmine, a dual-specific AChE and BChE inhibitor. The inhibition of ACh degradation results in increased endogenous levels of ACh. Treatment with rivastigmine started three weeks after transplantation, to avoid a possible inhibition of the acute rejection episode by increased ACh levels. A strong antiinflammatory effect of ACh on cells of the innate immune system has been documented before [177]. nAChRs are expressed by variety of leukocytes and other cytokine-producing cells [53] and ACh has been shown to decrease production of TNF-α, IL-1β, IL-6 and IL-18 by macrophages, but not antiinflammatory IL-10 via α-7 nicotinic receptors [178]. Additionally, α-7 subunit deficient mice are more susceptible to inflammatory stimuli such as lipopolysaccharide, and have higher serum levels of proinflammatory cytokines during inflammation [179]. The dose of rivastigmine, which was administered to the allograft recipients, has been previously shown to be effective [180]. Six months after transplantation, renal allografts were analysed histomorphometrically. Vascular remodelling is more prominent in rivastigmine-treated recipients compared with placebo-treated animals of healthy control kidneys. This holds true for all layers of the arterial wall including T. intima, T. media and T. adventitia. In addition to increased ACh levels, AChE inhibitors have been shown to interact with α-7 nicotinic receptors, and increase their expression [181].

In addition to increased ACh levels in the blood vessels of allografts, systemic treatment with rivastigmine probably also results in increased ACh levels in other parts of the body, which may induce a generalised vascular remodelling. To exclude that possibility, arteries in lungs and spleens were investigated and no significant differences between placebo and rivastigmine-treated recipients were found. These results highlight the importance of ACh locally released by intravascular allograft leukocytes. There is, however, a significant difference in the thickness of the lung arteries in placebo-treated animals compared with control animals. This could be due to animal ageing, as treated animals are 6 months older than control animals or to vascular remodelling caused by thrombi [166, 182], which may form after transplantation. It has been previously shown that thrombi may be involved in

forming neointimal hyperplasia [183]. Thrombi also have the properties to induce the accumulation of inflammatory cells and increase the release of proinflammatory cytokines [184].

Apart from intravascular graft leukocytes, other sources of ACh may contribute to vascular remodellling in allografts: endothelial cells, smooth muscle cells, infiltrating graft leukocytes, which all are immunopositive for ChAT and CHT1 in our immunohistochemical staining and have been described to produce ACH [185]. Another possible source of local ACh release - local neurons - can be excluded, because nerves are cut during transplantation.

On the basis of our data is tempting to propose the following steps in the pathogenesis of CAV: mononuclear leukocytes accumulate in close contact to allograft endothelial cells. These intravascular leukocytes are activated to produce ACh, which is released and acts in a paracrine fashion on nAChR expressed by allograft endothelia. In response to leukocytic ACh, endothelial cells proliferate and produce growth factors such as VEGF [186], which in turn mobilises VSMC from the media and promotes their proliferation. Smooth muscle cells may also be directly attracted by leukocytic ACh [186]. Both endothelial and smooth muscle cells contribute to the formation of intimal hyperplasia typical for CAV [166]. Similar processes may also happen in isografts. In isografts investigated in this study, presumably less ACh is released, which is quickly flushed away by the blood stream, because of the significantly lower number of leukocytes present in isografts.

5.9 Conclusions

In conclusion, our study demonstrates that leukocytes accumulating in the blood vessels of renal allografts undergoing chronic rejection produce ACh and that endogenous ACh contributes to the pathogenesis of CAV. Pharmacological targeting of vascular AChRs seems to be a promising strategy to prevent or cure chronic renal allograft rejection.

6. Summary

Leukocytes, which accumulate in graft blood vessels during fatal acute rejection of experimental renal allografts, synthesise and release acetylcholine (ACh). In this study, I tested the hypothesis that ACh produced by leukocytes accumulating in graft blood vessels contributes to the pathogenesis of chronic renal allograft vasculopathy (CAV).

Kidneys were transplanted in the allogeneic Fischer 344 to Lewis rat strain combination. Isogeneic transplantations were performed in Lewis rats. Intravascular graft leukocytes were investigated during an acute rejection episode on day 9 post-transplantation and during the process of vascular remodelling on day 42. The expression of essential elements for ACh synthesis and release was analysed by quantitative RT-PCR, Western blotting and immunohistochemistry. Furthermore, renal allograft recipients were treated with rivastigmine, an ACh-esterase inhibitor, or placebo.

Nine days after transplantation, numerous leukocytes accumulated in the blood vessels of the allograft (allograft: ~140 x 10^6; isograft: ~10 x 10^6). Leukocyte numbers decreased until day 42 after allogeneic transplantation (allograft: ~40 x 10^6; isograft: ~10 x 10^6). Within 6 months after transplantation, allografts developed typical hallmarks of chronic allograft injury - vascular remodelling, fibrosis, glomerular damage, tubular atrophy, and decreased renal function. The mRNA and protein expression of the high-affinity choline transporter was upregulated in allograft leukocytes on day 9 and day 42. Choline acetyltransferase (ChAT) mRNA was detected only sporadically. However, increased amounts of ChAT protein were detected in intravascular leukocytes from day 9 and 42 allografts compared with isografts. Carnitine acetyltransferase mRNA expression was increased in intravascular leukocytes from day 42 allografts compared with other groups. ACh itself was present at about the same level in leukocytes from isografts and allografts but absent in leukocytes from untreated kidneys. No vesicular acetylcholine transporter mRNA was detected but the mRNA of polyspecific organic cation transporters 1, 2, and 3 was present in all samples. In line with the hypothesis that endogenous ACh contributed to the pathogenesis of CAV, rivastigmine-treatment enhanced the severity of experimental CAV.

In conclusion, the results are in line with the hypothesis that leukocytic ACh contributes to the pathogenesis of CAV. The non-neuronal cholinergic system seems to be a promising target for the development of novel therapeutic approaches preventing CAV.

7. Zusammenfassung

Leukozyten, die sich während der akuten fatalen Abstoßung in den Blutgefäßen experimenteller Nierentransplantate ansammeln, produzieren Acetylcholin (ACh). In dieser Studie überprüfte ich die Hypothese, dass leukozytäres ACh zur Pathogenese der chronischen Transplantatvaskulopathie (CAV) beiträgt.

Nieren wurden in der allogenen Fischer 344 auf Lewis Rattenstammkombination transplantiert. Isogene Transplantate erfolgten in der Lewis-Ratte. Intravasale Transplantat-leukozyten wurden während einer akuten Abstoßungsepisode am 9. postoperativen Tag untersucht sowie während des Gefäßumbaus am Tag 42. Die Expression wesentlicher Elemente der ACh-Synthese und -Freisetzung wurde durch quantitative PCR, Western blotting und Immunhistochemie untersucht. Weiterhin wurden Empfänger allogener Transplantate mit Rivastigmin, einem ACH-Esteraseinhibitor oder mit Placebo behandelt.

Bis zum 9. postoperativen Tag sammelten sich zahlreiche Leukozyten in den Blutgefäßen der Transplantate an (allogenes Transplantat: ~140 x 10^6; isogenes Transplantat: ~10 x 10^6). Bis zum Tag 42 sanken die Leukozytenzahlen wieder, blieben jedoch im Vergleich zu entsprechenden isogenen Transplantaten vierfach erhöht (allogenes Transplantat: ~40 x 10^6; isogenes Transplantat: ~10 x 10^6). Innerhalb von 6 Monaten entwickelten die Transplantate typische Anzeichen der chronischen Transplantatschädigung – Gefäßumbau, Fibrose, Glomerulopathie, Tubulusatrophie und Funktionsstörung. An den Tagen 9 und 42 war die mRNA- und Proteinexpression des hochaffinen Cholintransporters hochreguliert. Die mRNA der Cholinacetyltransferase (ChAT) ließ sich nur sporadisch nachweisen. Hingegen war in Leukozyten aus allogenen Nierentransplantaten (Tag 9 und Tag 42) die Menge des ChAT-Proteins im Vergleich zu isogenen Transplantaten erhöht. Im Vergleich zu allen anderen Gruppen war die Expression der Carnitinacetyltransferase am Tag 42 nach allogener Transplantation erhöht. ACh selbst war etwa in gleicher Menge in Leukozyten aus isogenen und allogenen Transplantaten nachweisbar, jedoch nicht in Leukozyten aus unbehandelten Nieren. Die mRNA des vesikulären Acetylcholintransporters war nicht messbar, wohl aber die mRNA der organischen Cationentransporter-1, -2 und -3. In Übereinstimmung mit der Hypothese dass endogenes ACh zur Pathogenese der CAV beiträgt, verschlimmerte die Behandlung mit Rivastigmin den Schweregrad der CAV.

Die Ergebnisse sind folglich mit der Hypothese vereinbar, dass leukozytäres ACh zur Pathogenese der CAV beiträgt. Das non-neuronale cholinerge System scheint ein vielversprechender Ansatzpunkt zur Entwicklung neuer Therapien der CAV zu sein.

8. Literature

1. Axelrod, D.A., et al., *Kidney and pancreas transplantation in the United States, 1999-2008: the changing face of living donation.* Am J Transplant, 2010. **10**(4 Pt 2): p. 987-1002.
2. Wolfe, R.A., E.C. Roys, and R.M. Merion, *Trends in organ donation and transplantation in the United States, 1999-2008.* Am J Transplant, 2010. **10**(4 Pt 2): p. 961-72.
3. Helal, I., et al., *The first year renal function as a predictor of long-term graft survival after kidney transplantation.* Transplant Proc, 2009. **41**(2): p. 648-50.
4. Pascual, M., et al., *Strategies to improve long-term outcomes after renal transplantation.* N Engl J Med, 2002. **346**(8): p. 580-90.
5. Ansell, D. and C.R. Tomson, *UK Renal Registry 11th Annual Report (December 2008): Chapter 15 The UK Renal Registry, UKRR database, validation and methodology.* Nephron Clin Pract, 2009. **111 Suppl 1**: p. c277-85.
6. Libby, P. and J.S. Pober, *Chronic rejection.* Immunity, 2001. **14**(4): p. 387-97.
7. Seron, D., X. Fulladosa, and F. Moreso, *Risk factors associated with the deterioration of renal function after kidney transplantation.* Kidney Int Suppl, 2005(99): p. S113-7.
8. Aita, K., et al., *Peritubular capillaritis in early renal allograft is associated with the development of chronic rejection and chronic allograft nephropathy.* Clin Transplant, 2005. **19 Suppl 14**: p. 20-6.
9. Joosten, S.A., et al., *Chronic renal allograft rejection: pathophysiologic considerations.* Kidney Int, 2005. **68**(1): p. 1-13.
10. Lindholm, A., et al., *The impact of acute rejection episodes on long-term graft function and outcome in 1347 primary renal transplants treated by 3 cyclosporine regimens.* Transplantation, 1993. **56**(2): p. 307-15.
11. Pilmore, H.L., et al., *Early up-regulation of macrophages and myofibroblasts: a new marker for development of chronic renal allograft rejection.* Transplantation, 2000. **69**(12): p. 2658-62.
12. Opelz, G. and B. Dohler, *Influence of time of rejection on long-term graft survival in renal transplantation.* Transplantation, 2008. **85**(5): p. 661-6.
13. Massy, Z.A., et al., *Chronic renal allograft rejection: immunologic and nonimmunologic risk factors.* Kidney Int, 1996. **49**(2): p. 518-24.
14. Hostetter, T.H., *Chronic transplant rejection.* Kidney Int, 1994. **46**(1): p. 266-79.
15. Cosio, F.G., et al., *Transplant glomerulopathy.* Am J Transplant, 2008. **8**(3): p. 492-6.
16. Ivanyi, B., *Transplant capillaropathy and transplant glomerulopathy: ultrastructural markers of chronic renal allograft rejection.* Nephrol Dial Transplant, 2003. **18**(4): p. 655-60.
17. Mannon, R.B., *Therapeutic targets in the treatment of allograft fibrosis.* Am J Transplant, 2006. **6**(5 Pt 1): p. 867-75.
18. Rush, D., *Protocol biopsies for renal transplantation.* Saudi J Kidney Dis Transpl, 2010. **21**(1): p. 1-9.

19. Fotheringham, J., C.A. Angel, and W. McKane, *Transplant glomerulopathy: morphology, associations and mechanism.* Nephron Clin Pract, 2009. **113**(1): p. c1-7; discussion c7.
20. Paul, L.C., *Chronic allograft nephropathy: An update.* Kidney Int, 1999. **56**(3): p. 783-93.
21. Jevnikar, A.M. and R.B. Mannon, *Late kidney allograft loss: what we know about it, and what we can do about it.* Clin J Am Soc Nephrol, 2008. **3 Suppl 2**: p. S56-67.
22. Suzuki, J., et al., *Characteristics of chronic rejection in heart transplantation: important elements of pathogenesis and future treatments.* Circ J, 2010. **74**(2): p. 233-9.
23. Ramzy, D., et al., *Cardiac allograft vasculopathy: a review.* Can J Surg, 2005. **48**(4): p. 319-27.
24. Mehra, M.R., *Contemporary concepts in prevention and treatment of cardiac allograft vasculopathy.* Am J Transplant, 2006. **6**(6): p. 1248-56.
25. Cailhier, J.F., P. Laplante, and M.J. Hebert, *Endothelial apoptosis and chronic transplant vasculopathy: recent results, novel mechanisms.* Am J Transplant, 2006. **6**(2): p. 247-53.
26. Crosson, J.T., *Transplant rejection under the microscope.* Transplant Proc, 2007. **39**(3): p. 662-6.
27. Julius, B.K., et al., *Incidence, progression and functional significance of cardiac allograft vasculopathy after heart transplantation.* Transplantation, 2000. **69**(5): p. 847-53.
28. Chapman, J.R., *Longitudinal analysis of chronic allograft nephropathy: clinicopathologic correlations.* Kidney Int Suppl, 2005(99): p. S108-12.
29. Ahanchi, S.S., N.D. Tsihlis, and M.R. Kibbe, *The role of nitric oxide in the pathophysiology of intimal hyperplasia.* J Vasc Surg, 2007. **45 Suppl A**: p. A64-73.
30. Kang, D.H., et al., *Transplant graft vasculopathy: an emerging target for prevention and treatment of renal allograft dysfunction.* Yonsei Med J, 2004. **45**(6): p. 1053-8.
31. Choy, J.C., et al., *Perforin mediates endothelial cell death and resultant transplant vascular disease in cardiac allografts.* Am J Pathol, 2004. **165**(1): p. 127-33.
32. Ross, R., et al., *A platelet-dependent serum factor that stimulates the proliferation of arterial smooth muscle cells in vitro.* Proc Natl Acad Sci U S A, 1974. **71**(4): p. 1207-10.
33. Moreso, F., et al., *Serial protocol biopsies to quantify the progression of chronic transplant nephropathy in stable renal allografts.* Am J Transplant, 2001. **1**(1): p. 82-8.
34. Seron, D. and F. Moreso, *Transplant vasculopathy in early protocol renal allograft biopsies.* Transplant Proc, 1999. **31**(6): p. 2219-20.
35. Gloor, J.M., et al., *Transplant glomerulopathy: subclinical incidence and association with alloantibody.* Am J Transplant, 2007. **7**(9): p. 2124-32.
36. Pouteil-Noble, C., H. Maiza, and L. Remontet, *Post-transplant glomerular filtration rate as a marker for long-term outcome.* Ann Transplant, 2000. **5**(2): p. 29-36.
37. Seron, D., *Interstitial fibrosis and tubular atrophy in renal allograft protocol biopsies as a surrogate of graft survival.* Transplant Proc, 2009. **41**(2): p. 769-70.
38. Schwarz, A., et al., *Risk factors for chronic allograft nephropathy after renal transplantation: a protocol biopsy study.* Kidney Int, 2005. **67**(1): p. 341-8.
39. Nankivell, B.J., et al., *The natural history of chronic allograft nephropathy.* N Engl J Med, 2003. **349**(24): p. 2326-33.

40. Seron, D., et al., *Reliability of chronic allograft nephropathy diagnosis in sequential protocol biopsies.* Kidney Int, 2002. **61**(2): p. 727-33.
41. Nicholson, M.L., et al., *Early measurement of interstitial fibrosis predicts long-term renal function and graft survival in renal transplantation.* Br J Surg, 1996. **83**(8): p. 1082-5.
42. Diamond, J.R., et al., *Progressive albuminuria and glomerulosclerosis in a rat model of chronic renal allograft rejection.* Transplantation, 1992. **54**(4): p. 710-6.
43. Chandraker, A., et al., *Late blockade of T cell costimulation interrupts progression of experimental chronic allograft rejection.* J Clin Invest, 1998. **101**(11): p. 2309-18.
44. White, E., W.H. Hildemann, and Y. Mullen, *Chronic kidney allograft reactions in rats.* Transplantation, 1969. **8**(5): p. 602-17.
45. Gasser, M., et al., *Chronic rejection: insights from a novel immunosuppressive-free model of kidney transplantation.* J Am Soc Nephrol, 2004. **15**(3): p. 687-94.
46. Marco, M.L., *The Fischer-Lewis model of chronic allograft rejection--a summary.* Nephrol Dial Transplant, 2006. **21**(11): p. 3082-6.
47. Holler, J., et al., *Neuropeptide Y is expressed by rat mononuclear blood leukocytes and strongly down-regulated during inflammation.* J Immunol, 2008. **181**(10): p. 6906-12.
48. Hecker, A., et al., *Pivotal Advance: Up-regulation of acetylcholine synthesis and paracrine cholinergic signaling in intravascular transplant leukocytes during rejection of rat renal allografts.* J Leukoc Biol, 2009. **86**(1): p. 13-22.
49. Grau, V., et al., *Accumulating monocytes in the vasculature of rat renal allografts: phenotype, cytokine, inducible no synthase, and tissue factor mRNA expression.* Transplantation, 2001. **71**(1): p. 37-46.
50. Stehling, O., V. Grau, and B. Steiniger, *Monocyte cytotoxicity during acute kidney graft rejection in rats.* Int Immunol, 2004. **16**(1): p. 101-10.
51. Tayebati, S.K., et al., *Immunochemical and immunocytochemical characterization of cholinergic markers in human peripheral blood lymphocytes.* J Neuroimmunol, 2002. **132**(1-2): p. 147-55.
52. Fujii, T., Y. Takada-Takatori, and K. Kawashima, *Basic and clinical aspects of non-neuronal acetylcholine: expression of an independent, non-neuronal cholinergic system in lymphocytes and its clinical significance in immunotherapy.* J Pharmacol Sci, 2008. **106**(2): p. 186-92.
53. Kawashima, K. and T. Fujii, *The lymphocytic cholinergic system and its contribution to the regulation of immune activity.* Life Sci, 2003. **74**(6): p. 675-96.
54. Rinner, I., K. Kawashima, and K. Schauenstein, *Rat lymphocytes produce and secrete acetylcholine in dependence of differentiation and activation.* J Neuroimmunol, 1998. **81**(1-2): p. 31-7.
55. Fujii, T. and K. Kawashima, *An independent non-neuronal cholinergic system in lymphocytes.* Jpn J Pharmacol, 2001. **85**(1): p. 11-5.
56. Briscoe, D.M., S.I. Alexander, and A.H. Lichtman, *Interactions between T lymphocytes and endothelial cells in allograft rejection.* Curr Opin Immunol, 1998. **10**(5): p. 525-31.

57. Vos, I.H. and D.M. Briscoe, *Endothelial injury: cause and effect of alloimmune inflammation.* Transpl Infect Dis, 2002. **4**(3): p. 152-9.
58. Reinders, M.E., T.J. Rabelink, and D.M. Briscoe, *Angiogenesis and endothelial cell repair in renal disease and allograft rejection.* J Am Soc Nephrol, 2006. **17**(4): p. 932-42.
59. Al-Lamki, R.S., J.R. Bradley, and J.S. Pober, *Endothelial cells in allograft rejection.* Transplantation, 2008. **86**(10): p. 1340-8.
60. Wessler, I., et al., *The non-neuronal cholinergic system in humans: expression, function and pathophysiology.* Life Sci, 2003. **72**(18-19): p. 2055-61.
61. Dasgupta, P., et al., *Nicotine induces cell proliferation, invasion and epithelial-mesenchymal transition in a variety of human cancer cell lines.* Int J Cancer, 2009. **124**(1): p. 36-45.
62. Cooke, J.P. and Y.T. Ghebremariam, *Endothelial nicotinic acetylcholine receptors and angiogenesis.* Trends Cardiovasc Med, 2008. **18**(7): p. 247-53.
63. Egleton, R.D., K.C. Brown, and P. Dasgupta, *Nicotinic acetylcholine receptors in cancer: multiple roles in proliferation and inhibition of apoptosis.* Trends Pharmacol Sci, 2008. **29**(3): p. 151-8.
64. Lukas, R.J., et al., *International Union of Pharmacology. XX. Current status of the nomenclature for nicotinic acetylcholine receptors and their subunits.* Pharmacol Rev, 1999. **51**(2): p. 397-401.
65. Changeux, J.P., et al., *Brain nicotinic receptors: structure and regulation, role in learning and reinforcement.* Brain Res Brain Res Rev, 1998. **26**(2-3): p. 198-216.
66. Heeschen, C., et al., *Nicotine stimulates angiogenesis and promotes tumor growth and atherosclerosis.* Nat Med, 2001. **7**(7): p. 833-9.
67. Kilaru, S., et al., *Nicotine: a review of its role in atherosclerosis.* J Am Coll Surg, 2001. **193**(5): p. 538-46.
68. Conklin, B.S., et al., *Nicotine and cotinine up-regulate vascular endothelial growth factor expression in endothelial cells.* Am J Pathol, 2002. **160**(2): p. 413-8.
69. Pilmore, H.L., et al., *Vascular endothelial growth factor expression in human chronic renal allograft rejection.* Transplantation, 1999. **67**(6): p. 929-33.
70. Lemstrom, K.B., et al., *Vascular endothelial growth factor enhances cardiac allograft arteriosclerosis.* Circulation, 2002. **105**(21): p. 2524-30.
71. Raisky, O., et al., *VEGFR-1 and -2 regulate inflammation, myocardial angiogenesis, and arteriosclerosis in chronically rejecting cardiac allografts.* Arterioscler Thromb Vasc Biol, 2007. **27**(4): p. 819-25.
72. Kiuchi, K., et al., *Mecamylamine suppresses Basal and nicotine-stimulated choroidal neovascularization.* Invest Ophthalmol Vis Sci, 2008. **49**(4): p. 1705-11.
73. Patton, G.W., et al., *Nicotine modulation of cytokine induction by LPS-stimulated human monocytes and coronary artery endothelial cells.* Int Immunopharmacol, 2006. **6**(1): p. 26-35.
74. Saeed, R.W., et al., *Cholinergic stimulation blocks endothelial cell activation and leukocyte recruitment during inflammation.* J Exp Med, 2005. **201**(7): p. 1113-23.
75. Cirillo, P., et al., *Nicotine induces tissue factor expression in cultured endothelial and smooth muscle cells.* J Thromb Haemost, 2006. **4**(2): p. 453-8.

76. Aicher, A., et al., *Nicotine strongly activates dendritic cell-mediated adaptive immunity: potential role for progression of atherosclerotic lesions.* Circulation, 2003. **107**(4): p. 604-11.
77. Lau, P.P., et al., *Nicotine induces proinflammatory responses in macrophages and the aorta leading to acceleration of atherosclerosis in low-density lipoprotein receptor(-/-) mice.* Arterioscler Thromb Vasc Biol, 2006. **26**(1): p. 143-9.
78. Dasgupta, P. and S.P. Chellappan, *Nicotine-mediated cell proliferation and angiogenesis: new twists to an old story.* Cell Cycle, 2006. **5**(20): p. 2324-8.
79. Heeschen, C., et al., *A novel angiogenic pathway mediated by non-neuronal nicotinic acetylcholine receptors.* J Clin Invest, 2002. **110**(4): p. 527-36.
80. Mousa, S. and S.A. Mousa, *Cellular and molecular mechanisms of nicotine's pro-angiogenesis activity and its potential impact on cancer.* J Cell Biochem, 2006. **97**(6): p. 1370-8.
81. Zhu, B.Q., et al., *Second hand smoke stimulates tumor angiogenesis and growth.* Cancer Cell, 2003. **4**(3): p. 191-6.
82. Jacobi, J., et al., *Nicotine accelerates angiogenesis and wound healing in genetically diabetic mice.* Am J Pathol, 2002. **161**(1): p. 97-104.
83. Ng, M.K., et al., *A central role for nicotinic cholinergic regulation of growth factor-induced endothelial cell migration.* Arterioscler Thromb Vasc Biol, 2007. **27**(1): p. 106-12.
84. Costa, M.A., et al., *Role of cardiovascular nitric oxide system in C-type natriuretic peptide effects.* Biochem Biophys Res Commun, 2007. **359**(1): p. 180-6.
85. Rocha, A., I. Azevedo, and R. Soares, *Anti-angiogenic effects of imatinib target smooth muscle cells but not endothelial cells.* Angiogenesis, 2007. **10**(4): p. 279-86.
86. Benowitz, N.L., *Cigarette smoking and cardiovascular disease: pathophysiology and implications for treatment.* Prog Cardiovasc Dis, 2003. **46**(1): p. 91-111.
87. Ambrose, J.A. and R.S. Barua, *The pathophysiology of cigarette smoking and cardiovascular disease: an update.* J Am Coll Cardiol, 2004. **43**(10): p. 1731-7.
88. Lee, W.O. and S.M. Wright, *Production of endothelin by cultured human endothelial cells following exposure to nicotine or caffeine.* Metabolism, 1999. **48**(7): p. 845-8.
89. Salani, D., et al., *Endothelin-1 induces an angiogenic phenotype in cultured endothelial cells and stimulates neovascularization in vivo.* Am J Pathol, 2000. **157**(5): p. 1703-11.
90. Salani, D., et al., *Role of endothelin-1 in neovascularization of ovarian carcinoma.* Am J Pathol, 2000. **157**(5): p. 1537-47.
91. Wessler, I., et al., *The biological role of non-neuronal acetylcholine in plants and humans.* Jpn J Pharmacol, 2001. **85**(1): p. 2-10.
92. Lips, K.S., et al., *Polyspecific cation transporters mediate luminal release of acetylcholine from bronchial epithelium.* Am J Respir Cell Mol Biol, 2005. **33**(1): p. 79-88.
93. Wessler, I., C.J. Kirkpatrick, and K. Racke, *Non-neuronal acetylcholine, a locally acting molecule, widely distributed in biological systems: expression and function in humans.* Pharmacol Ther, 1998. **77**(1): p. 59-79.

94. Grando, S.A., et al., *Recent progress in understanding the non-neuronal cholinergic system in humans.* Life Sci, 2007. **80**(24-25): p. 2181-5.

95. Oda, Y., *Choline acetyltransferase: the structure, distribution and pathologic changes in the central nervous system.* Pathol Int, 1999. **49**(11): p. 921-37.

96. Kong, W.J., et al., *Ultrastructural localization of ChAT-like immunoreactivity in the human vestibular periphery.* Hear Res, 1998. **119**(1-2): p. 96-103.

97. Klapproth, H., et al., *Non-neuronal acetylcholine, a signalling molecule synthezised by surface cells of rat and man.* Naunyn Schmiedebergs Arch Pharmacol, 1997. **355**(4): p. 515-23.

98. Slemmon, J.R., P.M. Salvaterra, and E. Roberts, *Molecular characterization of choline acetyltransferase from Drosophila melanogaster.* Neurochem Int, 1984. **6**(4): p. 519-25.

99. Wu, D. and L.B. Hersh, *Choline acetyltransferase: celebrating its fiftieth year.* J Neurochem, 1994. **62**(5): p. 1653-63.

100. Misawa, H., K. Ishii, and T. Deguchi, *Gene expression of mouse choline acetyltransferase. Alternative splicing and identification of a highly active promoter region.* J Biol Chem, 1992. **267**(28): p. 20392-9.

101. Kengaku, M., H. Misawa, and T. Deguchi, *Multiple mRNA species of choline acetyltransferase from rat spinal cord.* Brain Res Mol Brain Res, 1993. **18**(1-2): p. 71-6.

102. Chireux, M.A., A. Le Van Thai, and M.J. Weber, *Human choline acetyltransferase gene: localization of alternative first exons.* J Neurosci Res, 1995. **40**(4): p. 427-38.

103. Cai, Y., et al., *Choline acetyltransferase structure reveals distribution of mutations that cause motor disorders.* EMBO J, 2004. **23**(10): p. 2047-58.

104. Prado, M.A., et al., *Regulation of acetylcholine synthesis and storage.* Neurochem Int, 2002. **41**(5): p. 291-9.

105. Fujii, T., et al., *Induction of choline acetyltransferase mRNA in human mononuclear leukocytes stimulated by phytohemagglutinin, a T-cell activator.* J Neuroimmunol, 1998. **82**(1): p. 101-7.

106. Wessler, I., C.J. Kirkpatrick, and K. Racke, *The cholinergic 'pitfall': acetylcholine, a universal cell molecule in biological systems, including humans.* Clin Exp Pharmacol Physiol, 1999. **26**(3): p. 198-205.

107. Kawashima, K. and T. Fujii, *Extraneuronal cholinergic system in lymphocytes.* Pharmacol Ther, 2000. **86**(1): p. 29-48.

108. Fujii, T., et al., *Localization and synthesis of acetylcholine in human leukemic T cell lines.* J Neurosci Res, 1996. **44**(1): p. 66-72.

109. Whittaker, V.P. and G.H. Dowe, *The Identification of the Acetylcholine-Like Substance in Synatosomes Derived from Guinea-Pig Brain as Acetylcholine Itself.* Int J Neuropharmacol, 1964. **3**: p. 593-7.

110. Fujii, T., et al., *Constitutive expression of mRNA for the same choline acetyltransferase as that in the nervous system, an acetylcholine-synthesizing enzyme, in human leukemic T-cell lines.* Neurosci Lett, 1999. **259**(2): p. 71-4.

111. Dobransky, T., et al., *Expression, purification and characterization of recombinant human choline acetyltransferase: phosphorylation of the enzyme regulates catalytic activity.* Biochem J, 2000. **349**(Pt 1): p. 141-51.

112. Auld, D.S., F. Mennicken, and R. Quirion, *Nerve growth factor rapidly induces prolonged acetylcholine release from cultured basal forebrain neurons: differentiation between neuromodulatory and neurotrophic influences.* J Neurosci, 2001. **21**(10): p. 3375-82.

113. Lips, K.S., et al., *Acetylcholine and molecular components of its synthesis and release machinery in the urothelium.* Eur Urol, 2007. **51**(4): p. 1042-53.

114. Michel, V., et al., *Choline transport for phospholipid synthesis.* Exp Biol Med (Maywood), 2006. **231**(5): p. 490-504.

115. Fujii, T., et al., *Acetylcholine synthesis and release in NIH3T3 cells coexpressing the high-affinity choline transporter and choline acetyltransferase.* J Neurosci Res, 2009. **87**(13): p. 3024-32.

116. Vickroy, T.W., et al., *Quantitative light microscopic autoradiography of [3H]hemicholinium-3 binding sites in the rat central nervous system: a novel biochemical marker for mapping the distribution of cholinergic nerve terminals.* Brain Res, 1985. **329**(1-2): p. 368-73.

117. Haga, T., *Synthesis and release of (14 C)acetylcholine in synaptosomes.* J Neurochem, 1971. **18**(6): p. 781-98.

118. Happe, H.K. and L.C. Murrin, *High-affinity choline transport sites: use of [3H]hemicholinium-3 as a quantitative marker.* J Neurochem, 1993. **60**(4): p. 1191-201.

119. Okuda, T. and T. Haga, *[The high-affinity choline transporter].* Tanpakushitsu Kakusan Koso, 2000. **45**(10): p. 1722-7.

120. Okuda, T. and T. Haga, *Functional characterization of the human high-affinity choline transporter.* FEBS Lett, 2000. **484**(2): p. 92-7.

121. Okuda, T., et al., *Identification and characterization of the high-affinity choline transporter.* Nat Neurosci, 2000. **3**(2): p. 120-5.

122. Apparsundaram, S., et al., *Molecular cloning of a human, hemicholinium-3-sensitive choline transporter.* Biochem Biophys Res Commun, 2000. **276**(3): p. 862-7.

123. Apparsundaram, S., S.M. Ferguson, and R.D. Blakely, *Molecular cloning and characterization of a murine hemicholinium-3-sensitive choline transporter.* Biochem Soc Trans, 2001. **29**(Pt 6): p. 711-6.

124. Okuda, T. and T. Haga, *High-affinity choline transporter.* Neurochem Res, 2003. **28**(3-4): p. 483-8.

125. Pfeil, U., et al., *Expression of the high-affinity choline transporter CHT1 in epithelia.* Life Sci, 2003. **72**(18-19): p. 2087-90.

126. Pfeil, U., et al., *Expression of the high-affinity choline transporter, CHT1, in the rat trachea.* Am J Respir Cell Mol Biol, 2003. **28**(4): p. 473-7.

127. Lips, K.S., et al., *Expression of the high-affinity choline transporter CHT1 in rat and human arteries.* J Histochem Cytochem, 2003. **51**(12): p. 1645-54.

128. Fujii, T., et al., *Detection of the high-affinity choline transporter in the MOLT-3 human leukemic T-cell line.* Life Sci, 2003. **72**(18-19): p. 2131-4.

129. Misawa, H., R. Takahashi, and T. Deguchi, *Coordinate expression of vesicular acetylcholine transporter and choline acetyltransferase in sympathetic superior cervical neurones.* Neuroreport, 1995. **6**(7): p. 965-8.

130. Usdin, T.B., et al., *Molecular biology of the vesicular ACh transporter.* Trends Neurosci, 1995. **18**(5): p. 218-24.

131. Arvidsson, U., et al., *Vesicular acetylcholine transporter (VAChT) protein: a novel and unique marker for cholinergic neurons in the central and peripheral nervous systems.* J Comp Neurol, 1997. **378**(4): p. 454-67.

132. Elwary, S.M., B. Chavan, and K.U. Schallreuter, *The vesicular acetylcholine transporter is present in melanocytes and keratinocytes in the human epidermis.* J Invest Dermatol, 2006. **126**(8): p. 1879-84.

133. Kummer, W., et al., *Role of acetylcholine and polyspecific cation transporters in serotonin-induced bronchoconstriction in the mouse.* Respir Res, 2006. **7**: p. 65.

134. Koepsell, H., K. Lips, and C. Volk, *Polyspecific organic cation transporters: structure, function, physiological roles, and biopharmaceutical implications.* Pharm Res, 2007. **24**(7): p. 1227-51.

135. Johnson, C.D. and R.L. Russell, *Multiple molecular forms of acetylcholinesterase in the nematode Caenorhabditis elegans.* J Neurochem, 1983. **41**(1): p. 30-46.

136. Koelle, G.B., et al., *Anticholinesterase Agents.* Science, 1963. **141**(3575): p. 63-5.

137. Adler, M., et al., *Regulation of acetylcholine hydrolysis in canine tracheal smooth muscle.* Eur J Pharmacol, 1991. **205**(1): p. 73-9.

138. Norel, X., et al., *Degradation of acetylcholine in human airways: role of butyrylcholinesterase.* Br J Pharmacol, 1993. **108**(4): p. 914-9.

139. Cooke, J.R., et al., *Acetylcholinesterase inhibitors and sleep architecture in patients with Alzheimer's disease.* Drugs Aging, 2006. **23**(6): p. 503-11.

140. Farlow, M.R., *Update on rivastigmine.* Neurologist, 2003. **9**(5): p. 230-4.

141. Williams, B.R., A. Nazarians, and M.A. Gill, *A review of rivastigmine: a reversible cholinesterase inhibitor.* Clin Ther, 2003. **25**(6): p. 1634-53.

142. Fabre, J., S.H. Lim, and P.J. Morris, *Renal transplantation in the rat: details of a technique.* Aust N Z J Surg, 1971. **41**(1): p. 69-75.

143. Wilczynska, J., et al., *Acetylcholine and chronic vasculopathy in rat renal allografts.* Transplantation, 2011. **91**(3): p. 263-70.

144. Mahabir, R.N., R.D. Guttmann, and R.R. Lindquist, *Renal transplantation in the inbred rat. X. A model of "weak histoincompatibility" by major locus matching.* Transplantation, 1969. **8**(4): p. 369-78.

145. Hancock, W.H., et al., *Cytokines, adhesion molecules, and the pathogenesis of chronic rejection of rat renal allografts.* Transplantation, 1993. **56**(3): p. 643-50.

146. Joosten, S.A., C. van Kooten, and L.C. Paul, *Pathogenesis of chronic allograft rejection.* Transpl Int, 2003. **16**(3): p. 137-45.

147. Calne, R.Y., et al., *Cyclosporin A in patients receiving renal allografts from cadaver donors.* Lancet, 1978. **2**(8104-5): p. 1323-7.

148. Morris, P.J., et al., *Cyclosporin conversion versus conventional immunosuppression: long-term follow-up and histological evaluation.* Lancet, 1987. **1**(8533): p. 586-91.

149. Chapman, J.R., et al., *Reversibility of cyclosporin nephrotoxicity after three months' treatment.* Lancet, 1985. **1**(8421): p. 128-30.

150. Hall, B.M., et al., *Comparison of three immunosuppressive regimens in cadaver renal transplantation: long-term cyclosporine, short-term cyclosporine followed by azathioprine and prednisolone, and azathioprine and prednisolone without cyclosporine.* N Engl J Med, 1988. **318**(23): p. 1499-507.

151. Myers, B.D., et al., *Cyclosporine-associated chronic nephropathy.* N Engl J Med, 1984. **311**(11): p. 699-705.

152. Palestine, A.G., et al., *Renal histopathologic alterations in patients treated with cyclosporine for uveitis.* N Engl J Med, 1986. **314**(20): p. 1293-8.

153. Farnsworth, A., et al., *Interstitial fibrosis in renal allografts in patients treated with cyclosporin.* Lancet, 1984. **2**(8417-8418): p. 1470-1.

154. Homan, W.P., et al., *Studies on the effects of cyclosporin A upon renal allograft rejection in the dog.* Surgery, 1980. **88**(1): p. 168-73.

155. He, Z., et al., *Conversion from cyclosporin A to sirolimus retards the progression of chronic allograft nephropathy in the long term in a rat kidney transplantation model.* J Int Med Res, 2009. **37**(5): p. 1396-410.

156. Zakrzewicz, A., et al., *Leukocyte accumulation in graft blood vessels during self-limiting acute rejection of rat kidneys.* Immunobiology. 2011. **216**(5): p. 613-24. Epub 2010 Sep 24.

157. Azuma, H., et al., *Cellular and molecular predictors of chronic renal dysfunction after initial ischemia/reperfusion injury of a single kidney.* Transplantation, 1997. **64**(2): p. 190-7.

158. Torras, J., et al., *Long-term protective effect of UR-12670 after warm renal ischemia in uninephrectomized rats.* Kidney Int, 1999. **56**(5): p. 1798-808.

159. Andriambeloson, E., et al., *Transplantation-induced functional/morphological changes in rat aorta allografts differ from those in arteries of rat kidney allografts.* Am J Transplant, 2004. **4**(2): p. 188-95.

160. Beckmann, N., et al., *Macrophage labeling by SPIO as an early marker of allograft chronic rejection in a rat model of kidney transplantation.* Magn Reson Med, 2003. **49**(3): p. 459-67.

161. Bedke, J., et al., *Beneficial effects of CCR1 blockade on the progression of chronic renal allograft damage.* Am J Transplant, 2007. **7**(3): p. 527-37.

162. Gonzalez, M.C., et al., *Effect of removal of adventitia on vascular smooth muscle contraction and relaxation.* Am J Physiol Heart Circ Physiol, 2001. **280**(6): p. H2876-81.

163. Laflamme, K., et al., *Adventitia contribution in vascular tone: insights from adventitia-derived cells in a tissue-engineered human blood vessel.* FASEB J, 2006. **20**(8): p. 1245-7.

164. Davis, S.F., et al., *Early endothelial dysfunction predicts the development of transplant coronary artery disease at 1 year posttransplant.* Circulation, 1996. **93**(3): p. 457-62.

165. Simonson, M.S., et al., *Elevated neointimal endothelin-1 in transplantation-associated arteriosclerosis of renal allograft recipients.* Kidney Int, 1998. **54**(3): p. 960-71.

166. Mitchell, R.N. and P. Libby, *Vascular remodeling in transplant vasculopathy.* Circ Res, 2007. **100**(7): p. 967-78.

167. Tucek, S., *The synthesis of acetylcholine in skeletal muscles of the rat.* J Physiol, 1982. **322**: p. 53-69.

168. Yabuki, M., et al., *Molecular and functional characterization of choline transporter in rat renal tubule epithelial NRK-52E cells.* Arch Biochem Biophys, 2009. **485**(1): p. 88-96.

169. Horiuchi, Y., et al., *Evolutional study on acetylcholine expression.* Life Sci, 2003. **72**(15): p. 1745-56.

170. Jaffe, M.J., *Evidence for the regulation of phytochrome-mediated processes in bean roots by the neurohumor, acetylcholine.* Plant Physiol, 1970. **46**(6): p. 768-77.

171. Wessler, I., et al., *Release of non-neuronal acetylcholine from the isolated human placenta is mediated by organic cation transporters.* Br J Pharmacol, 2001. **134**(5): p. 951-6.

172. Wessler, I., et al., *Release of non-neuronal acetylcholine from the human placenta: difference to neuronal acetylcholine.* Naunyn Schmiedebergs Arch Pharmacol, 2001. **364**(3): p. 205-12.

173. Okuda, M., et al., *Molecular mechanisms of organic cation transport in OCT2-expressing Xenopus oocytes.* Biochim Biophys Acta, 1999. **1417**(2): p. 224-31.

174. Koepsell, H., B.M. Schmitt, and V. Gorboulev, *Organic cation transporters.* Rev Physiol Biochem Pharmacol, 2003. **150**: p. 36-90.

175. Lips, K.S., et al., *Down-regulation of the non-neuronal acetylcholine synthesis and release machinery in acute allergic airway inflammation of rat and mouse.* Life Sci, 2007. **80**(24-25): p. 2263-9.

176. Schlereth, T., et al., *In vivo release of non-neuronal acetylcholine from the human skin as measured by dermal microdialysis: effect of botulinum toxin.* Br J Pharmacol, 2006. **147**(2): p. 183-7.

177. Tracey, K.J., *Physiology and immunology of the cholinergic antiinflammatory pathway.* J Clin Invest, 2007. **117**(2): p. 289-96.

178. Borovikova, L.V., et al., *Vagus nerve stimulation attenuates the systemic inflammatory response to endotoxin.* Nature, 2000. **405**(6785): p. 458-62.

179. van Maanen, M.A., et al., *Role of the cholinergic nervous system in rheumatoid arthritis: aggravation of arthritis in nicotinic acetylcholine receptor alpha7 subunit gene knockout mice.* Ann Rheum Dis, 2010. **69**(9): p. 1717-23.

180. Scali, C., et al., *Effect of subchronic administration of metrifonate, rivastigmine and donepezil on brain acetylcholine in aged F344 rats.* J Neural Transm, 2002. **109**(7-8): p. 1067-80.

181. Reid, R.T. and M.N. Sabbagh, *Effects of cholinesterase inhibitors on rat nicotinic receptor levels in vivo and in vitro.* J Neural Transm, 2008. **115**(10): p. 1437-44.

182. Spencer, J.A., et al., *Altered vascular remodeling in fibulin-5-deficient mice reveals a role of fibulin-5 in smooth muscle cell proliferation and migration.* Proc Natl Acad Sci U S A, 2005. **102**(8): p. 2946-51.

183. Torsney, E., et al., *Thrombosis and neointima formation in vein grafts are inhibited by locally applied aspirin through endothelial protection.* Circ Res, 2004. **94**(11): p. 1466-73.

184. Kazi, M., et al., *Influence of intraluminal thrombus on structural and cellular composition of abdominal aortic aneurysm wall.* J Vasc Surg, 2003. **38**(6): p. 1283-92.

185. Wessler, I. and C.J. Kirkpatrick, *Acetylcholine beyond neurons: the non-neuronal cholinergic system in humans.* Br J Pharmacol, 2008. **154**(8): p. 1558-71.

186. Li, S., et al., *Nicotinic acetylcholine receptor alpha7 subunit mediates migration of vascular smooth muscle cells toward nicotine.* J Pharmacol Sci, 2004. **94**(3): p. 334-8.

187. Hecker, A., et al., *Peripheral choline acetyltransferase is expressed by monocytes and upregulated during renal allograft rejection in rats.* J Mol Neurosci, 2006. **30**(1-2): p. 23-4.

9. Declaration

"I declare that I have completed this dissertation single-handedly without the unauthorized help of a second party and only with the assistance acknowledged therein. I have appropriately acknowledged and referenced all text passages that are derived literally from or are based on the content of published or unpublished work of others, and all information that relates to verbal communications. I have abided by the principles of good scientific conduct laid down in the charter of the Justus Liebig University of Giessen in carrying out the investigations described in the dissertation."

Giessen, 13.04.2011 Joanna Wilczynska

Der Lebenslauf wurde aus der elektronischen Version der Arbeit entfernt.

The curriculum vitae was removed from the electronic version of the paper.

11. Acknowledgements

Writing a doctoral thesis was a challenging and long-lasting process. I would like to thank the many people that have made the completion of this dissertation possible.

This thesis would not have been possible without the help and support of my supervisor, Prof. Veronika Grau. I would like to thank her for her patience, motivation, enthusiasm, and immense knowledge. I could not have imagined having a better advisor and mentor for my PhD study. My sincere thanks go to Prof. Wolfgang Kummer for offering me the cooperation opportunities in his group and leading me to work with wonderful people. I would like to thank my co-workers and friends from Laboratory of Experimental Surgery: Sigrid Wilker, Petra Freitag, Gabi Fuch-Moll, Renate Plaß and Kathrin Petri for practical and teoretical help. I also want to thank my co-workers from Anatomy and Cell Biology Department: Silke Wiegand, Uwe Pfeil and Miriam Wolff for help, ideas and guiding me through the maze of the building's corridors .

Special thanks go to dr. Anna Zakrzewicz and dr. Dariusz Zakrzewicz for friendship, support during my research, intriguing conversations and time spent together. I also thank all my friends: Marta Kosinska, Ewa Jablonska, Aleksandra Tecza and Ewa Kolosionek for all the free anti-stress therapy that I have received from them.

My warmest gratitude goes to my partner Klaus. Thank you for your support, encouragement and companionship. You are my windshield against all storms.

Foremost I would like to thank my parents. For believing in me, always being there when I needed them most, and never once complaining about how infrequently I visit them. They deserve far more credit than I can ever give them.

Thank you all for your insights, guidance and support!

édition scientifique
VVB LAUFERSWEILER VERLAG

VVB LAUFERSWEILER VERLAG
STAUFENBERGRING 15
D-35396 GIESSEN

Tel: 0641-5599888 Fax: -5599890
redaktion@doktorverlag.de
www.doktorverlag.de

ISBN: 978-3-8359-5816-6